

SL. No 27

Flow and Heat Transfer Characteristics of Wall Jet over Rough Surfaces

by

Md. Golam Kader

This thesis is submitted to the Department of MECHANICAL
ENGINEERING in partial fulfillment of the requirements for the
award of the degree of

Master of Engineering

In

Mechanical Engineering



Bangladesh Institute of Technology, Khulna.
January, 2003.

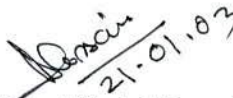
Bangladesh Institute of Technology, Khulna.
Department of Mechanical Engineering

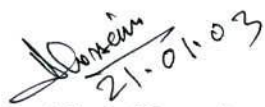
We here by recommend that project report prepared by


Md. Golam Kader


**“ Flow and Heat Transfer Characteristics of Wall Jet
Over Rough Surfaces”.**

Be accepted as fulfilling this part of the requirements for the degree of Master of
Engineering (Mechanical Engineering).


21.01.03
Professor **Dr. Khandkar Aftab Hossain** **Chairman**
Head, Mechanical Engineering Department
Bangladesh Institute of Technology, Khulna.


21.01.03
Professor **Dr. Khandkar Aftab Hossain** **Member
(Supervisor)**
Mechanical Engineering Department
Bangladesh Institute of Technology, Khulna.


21.01.03
Professor **Dr. Md. Nawsher Ali Moral.** **Member**
Mechanical Engineering Department
&
Director
Bangladesh Institute of Technology, Khulna.


Professor **Dr. M.A. Rashid Sarkar** **Member
(External)**
Mechanical Engineering Department
Bangladesh University of Engineering and Technology,
Dhaka.

January, 2003.

CERTIFICATE OF RESEARCH

This is to certify that the work presented in this thesis is out come of the investigation carried out by the candidate under the supervision of Dr. Khandkar Aftab Hossain, Professor and Head of the Department of Mechanical Engineering, B.I.T., Khulna, Bangladesh.



SUPERVISOR



CANDIDATE

DECLARATION

This is to certify that I have done this work and it was not submitted elsewhere for the award of any degree or diploma or for any publication.

Countersigned by


(Supervisor)

Author


(Md. Golam Kader)

ACKNOWLEDGEMENT

Bismillahir Rahmanir Rahim.

At the beginning of writing the acknowledgement I pay my shukria to Almighty Allah, with his blessings have succeeded in completing this thesis.

The author is deeply indebted and much obliged to Professor Dr. Khandkar Aftab Hossain, for his valuable suggestions, inspiration, guidance and constant encouragement in carrying out this research work. The author is very much grateful to Professor Dr. Naseem Ahmed, Director BIT, Dhaka, for his kind help at various stages of this research work and for the helpful discussion. The author also wishes to thanks Dr. A. N.M. Mizanur Rahman, Professor and Mr. Md. Ashraful Alam, Lecturer of this Department for their inspiration.

Thanks are also due to Professor Dr. Md. Nawsher Ali Moral, Director, BIT, Khulna for his inspiration.

Appreciation also goes to Mr. Monirul Azim, Mr. Md. Tabarak Hossain and other staff member in the Department for their kind help in different stages of this project work.

At last the author expresses sincere gratitude to his wife and daughters for their encouragement and kind help during this work.

Date.....

Author

DEDICATED
TO MY DAUGHTERS

ABSTRACT

Experimental investigation were carried out to verify the pressure distribution and the local Nusselt number due to circular wall jet over uniformly heated rough flat surfaces. The present investigation shows the dependence of the pressure on jet exit Reynolds number and relative roughness of the surfaces. It was observed that the overall pressure co-efficient, C_p decreases with the increase of jet exit Reynolds number and also decreases with the increase of surface roughness. The present investigation shows the local Nusselt number distribution with various Reynolds number and relative roughness of the surfaces. Jet exit Reynolds numbers of 8799, 10777, 16849 and 18804 as well as relative surface roughness of smooth, 0.01371, 0.01435, 0.01581 and 0.01613 were considered for this investigation.

The coefficient of pressure decreases with the increase of jet exit Reynolds number because of the fluid moving with higher kinetic energy initially and decays along the length of the surface due to frictional effect and decreases with the increase of relative surface roughness because the effect of friction increases with the increase of relative roughness. It was observed that the local Nusselt number increases with the increase of jet exit Reynolds number and also increases with the increase of surface roughness. Because of higher Reynolds number turbulence is generated in the laminar sub-layer, which is mixed in the buffer layer of the boundary layer.

The average Nusselt number was calculated and a correlation developed in terms of jet Reynolds number and relative roughness of the surface. The correlation yields $\pm 10\%$ accuracy with experimental findings.

Experimental results provided useful information, which have significant and potential industrial applications regarding the heat transfer area and surface roughness for maximizing the average Nusselt number.

TABLE OF CONTENTS

	<u>TITLE</u>	<u>PAGE</u>
	Certificate of Research	iii
	Declaration	iv
	Acknowledgement	v
	Abstract	vii
	Table of Contents	ix
	Nomenclature	xi
	List of Figures	xii
CHAPTER I	INTRODUCTION	
1.1	General Discussion	01
1.2	Flow Phenomena	02
1.3	Fluid Mechanics of Jet	04
1.3.1.1	Confined or Bounded jet	04
1.3.1.2	Wall jet	04
1.3.1.3	Free jet	06
1.3.1.4	Plane jet	07
1.3.1.5	Axisymmetric jet	07
1.3.1.6	Cross flow jet	07
1.4	Surface roughness and its measurement	08
1.5	Classification of Rough surfaces	08
1.6	Objectives of the study	10
CHAPTER II	LITERATURE REVIEW	
2.1	General	11

	<u>TITLE</u>	<u>PAGE</u>
CHAPTER III METHODOLOGY		
3.1	Calculation of Surface Roughness	24
3.2	Experimental set-up	25
3.2.1	Air jet and pressure measuring arrangement	25
3.2.2	Jet support arrangement	26
3.2.3	Heater assembly including test surfaces	26
3.2.4	Temperature measuring arrangement	27
3.3	Experimental technique	27
3.4	Error Analysis	28
CHAPTER IV RESULTS AND DISCUSSION		
4.1	General Discussion	32
4.2	Pressure Distribution	32
4.2.1	Effect of Reynolds number on Pressure distribution	32
4.2.2	Effect of Surface Roughness on pressure distribution	33
4.3	Heat transfer characteristics	34
4.3.1	Effect of Reynolds number on heat transfer characteristics	34
4.3.2	Effect of surface roughness on heat transfer characteristics	35
4.4	Correlation of Average Nusselt number	36
CHAPTER V CONCLUSION		
5.1	Conclusion for pressure distribution	38
5.2	Conclusion for heat transfer characteristics	39
5.3	Scope of further work	40
	REFERENCES	62
	APPENDIX A	67

NOMENCLATURE

A	Heat transfer area, in m ² .
C _p	Co-efficient of Pressure, $\frac{(P-P_a)}{2 \rho v_j^2}$
d	Jet diameter in m.
dx	Distance between two adjacent points on rough surface in m.
k _f	Thermal conductivity of fluid (air). (W/m.- K)
k _s	Thermal conductivity of surface.
$\overline{Nu_x}$	Local Nusselt No, $\frac{q \cdot dx}{k_a (T - T_j)}$
Nu	Average Nusselt number,
P - P _a	Measured pressure, kN/m ² .
P _r	Prandtl number, $\frac{\mu C_p}{k_f}$
q	Surface heat flux (kW/m ²).
Re	Reynolds number based on the diameter of the jet, $\frac{vd}{\gamma}$
R _a	Center line average roughness, in μm.
r _o	Radius of the jet, in m.
T _j	Temperature of air jet K.
T _w	Local temperature of the heat transfer surface K.
T	Local temperature after jet impingement K.
T ₁	Temperature of heated surface at point 1.
T ₂	Temperature of heated surface at point 2.
U _x	Velocity of fluid along the length of the surface.
v	Velocity of air jet in m/sec
X	Non dimensional length along the jet, $\frac{x}{d}$
x	Length along the jet, in m.

GREEK ALPHABETS

ε	Dimensionless relative roughness, $\frac{R_a}{d}$
θ	Dimensionless temperature, $\frac{(T - T_j)^d}{T_w - T_j}$
ρ	Air density in kg/m ³ .
μ	Dynamic viscosity of air in N-sec/m ²
ν	Kinematic viscosity of air in m ² /sec.
γ	Specific weight of manometric fluid N/m ³ .

LIST OF FIGURES

Figures No.	Description	Page No.
1.1	Wall jet over a solid surface	03
1.2	Wall jet with two distinct regions	04
3.1	Schematic diagram of Experimental Setup	41
3.2	M.S. Sheet test section	42
4.1.1	Distribution of co-efficient of pressure, C_p along the length of the smooth surface at various Reynolds numbers Re .	43
4.1.2 to 4.1.5	Distributions of co-efficient of pressure C_p over surfaces of different roughness for various jet exit Reynolds number.	44-47
4.1.6 to 4.1.9	Distributions of co-efficient of pressure C_p over long the length of the surfaces at different jet exit Reynolds number.	48-51
4.1.10	Distribution of Nusselt number for different Reynolds number over smooth surface .	52
4.1.11 to 4.1.14	Distribution of Nusselt number for different Reynolds number over different rough surface .	53-56
4.1.15 to 4.1.18	Distribution of Nusselt number for a specific Reynolds number over the surfaces of different roughness .	57-60
4.2.	Calculated Average Nusselt Numbr Vs. Experimental Average Nusselt Number plot.	61



CHAPTER - I

INTRODUCTION

1.1. General :

Circular wall Jet is a common method of heating or cooling the solid surfaces. Heat transfer in wall jet is generally superior to that of conventional methods. Because, fluid flow in the form of wall jets increases the momentum. In turbulent flow, the molecules in the flowing fluid are moving in a random manner. The molecules of flowing fluid transfer momentum and energy from one place to another by mixing of the fluid particle typically termed as eddy mixing. Generally, the rate of heat transfer is high in turbulent flow because of increased and random mixing. Thus, most practical application of wall jet occur in industries, where the heat transfer requirements have exceeded the capacity of ordinary heating and cooling techniques. Wall jet may also be used for controlled heating and cooling. Industrial wall jet includes, drying of paper, textiles and veneer, tempering of glass, annealing of metals and cooling of gas turbine blades, electronic components and drying of films in film industries.

Investigations have been reported in last few decades emphasized on various aspects of fluid mechanics and heat transfer of wall jet.

However, most of the earlier studies are confined with wall jet on smooth surfaces. Recently, wall jet on arrays of block mounted on other flat surfaces has attracted considerable attention. Many investigators have observed that relatively high heat transfer characteristics of wall jet are associated with high level of turbulence in the flow of fluid. A variety of turbulence promoting schemes have been used to enhance heat transfer. The new investigation of plane wall jet combined with extended and modified surfaces have shown promising results. The present study has been encountered to investigate the pressure distribution and heat transfer characteristics due to flow of circular wall jet over flat smooth and flat rough surfaces. In this case, heat transfer between uniformly heated rough flat surfaces and circular wall jet was investigated experimentally to determine the values of local and average Nusselts numbers and pressure distribution.

1.2 Flow Phenomena :

The jet of fluid with high kinetic energy exit from a nozzle of relatively narrow diameter hole than the tube diameter through which the blower supplying the fluid. Before exiting the nozzle tip the fluid has the high pressure. But after exiting the nozzle tip the fluid moving with high velocity and then the pressure remains at atmospheric. In the present investigation the fluid with high kinetic energy exit from the nozzle

and flows over the solid surface. As a result the velocity of fluid reduces in contact with the solid surface and boundary layer will develop. The following figure will show the fluid flow phenomena for wall jet over a solid surface.

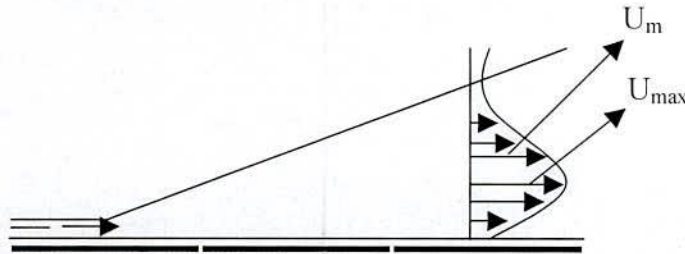


Figure 1.1 Wall Jet over a solid surface.

The jet of fluid flows along the surface and gradually boundary layer develops, but at the leading edge the jet has high velocity. Above the jet boundary the fluid is stagnant with atmospheric pressure. After the flow of jet, the surrounding fluid will move and energy is transferred from the jet to the surrounding fluid. As a result, the jet of fluid decays gradually. The maximum velocity of the jet decreases with $X^{-\frac{1}{2}}$ width of the jet increases with the increase of x , where x is the distance from the nozzle exit.

The wall jet composed of two regions, one is the inner region and the other is the outer region. The inner region is near the wall and similar to the flow of boundary layer flow with zero pressure gradient.



Whereas, the outer region is similar to the free jet flow. The typical velocity profile is shown below with two distinct regions.

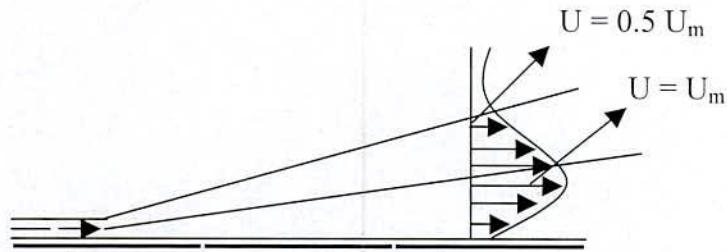


Figure 1.2 Wall jet with two distinct regions.

1.3 Fluid Mechanics of Jet :

A jet is created by the flow of fluid through an orifice or a nozzle into the stagnant reservoir or co-current stream of fluids. Jets are of three types, namely,

1. Confined or Bounded jet
2. Wall jet
3. Free jet

1.3.1 Confined or Bounded jet :

In the case of bounded jet the fluid is discharged from a nozzle or an orifice into a confined region bounded by solid surfaces. So, no entrainment will add to the main stream.

1.3.2 Wall jet :

When a jet spreads over a surface into surroundings of similar composition as the jet it is called wall jet. If it spreads in one direction on a plane surface, it is called plane wall jet and if it spreads radially in

wall direction, it is called radial wall jet, wall jets also constitute part of more complex flows as in impinging jets. When a jet of fluid impinges on a solid surface at an angle, four regions are observed, namely, free jet regime, stagnation regime, transition regime and the wall jet regime. Wall jet region is a fully developed boundary layer region in which the velocity is zero at the solid surface and at the outer edge of the jet with a maximum value in the interior. The jet momentum does not remain constant as in free jets. Tetervin first examined Laminar plane wall jet theoretically. Schwarz and Cosart have measured the velocity distributions for the incompressible, turbulent, plane wall jet and the variation of the velocity and length scales in the downstream direction. It has been reported that all mean velocity data can be reduced to a single universal curve with the length scale, x and the velocity scale U_m . It has been observed that the velocity scale varies as a power of x with an exponent -0.555 and the length scale with 1. Empirical expressions have been developed to correlate the length and velocity scales with nozzle exit velocity, nozzle width and the physical properties of the fluid. The $\overline{u'v'}$ correlation has been given as a function of the distance from the wall. This is computed from the mean velocity data assuming self-preserving characteristics.

1.3.3 Free jet :

It forms when the jet flows in an infinite fluid reservoir having no influence or contact of solid surface after exit. A brief description of free jet and jet impingement is given here for clarification of the discussions to follow.

The jet emanates from a nozzle with a velocity greater than that of the surrounding fluid, which may be stagnant also. The jet at its outer periphery comes into contact with surrounding fluid and tries to drag it along in the streaming direction, that is, imparts momentum to it. This sets the surrounding fluid in motion, since by continuity the fluid, which has been dragged, must be replaced by fluid coming towards the jet from outer boundaries. It is called entrainment. In this process, the jet fluid loses its momentum and energy. The centreline velocity of the jet upto some axial distance is not affected by mixing and diffusion occurring at its periphery. This unaffected region of jet is called potential core. The flow in potential core is unaffected by viscosity and its length depends upon Reynolds number.

The centerline velocity decreases beyond the potential core in the axial direction. The rate of decay of centre line velocity away from the potential core region for laminar slot jet is proportional to $(x/w)^{-1/3}$ and for laminar axisymmetric jet. It is proportional to $(x/d)^{-1}$. The pressure

and the total momentum of the jet remain constant along the main flow direction. The temperature of the warm jet injected into cold surrounding fluid, decreases due to the diffusion and due to the entrainment of surrounding cold fluid. The decay of non-dimensional centreline temperature is also proportional to $(x/w)^{-1/3}$ for laminar slot jet and $(x/d)^{-1}$ for laminar axisymmetric jet just like the decay of centreline velocity. The potential core for temperature depends upon the Reynolds number and Prandtl's number. Laminar jet at low Reynolds number is essentially a dissipated jet in which large viscous forces cause rapid diffusion of the jet into surrounding fluid. Entrainment will influence the main flow stream. Free jets are:

1.3.3.1 Plane jet :

Fluid is discharged from a plane nozzle of large length into a large stagnant mass of the same fluid.

1.3.3.2 Axisymmetric jet :

Fluid is discharged from a circular nozzle, orifice or pipe into a large stagnant mass of the same fluid. The jet spreads axially and radially in the surrounding fluid only.

1.3.3.3 Cross flow jet :

Any free jet when discharged in a moving stream of fluid whose direction is other than parallel to the axis of the jet.

1.4 Surface roughness and its measurement :

A little consideration will show that surfaces produced by different machining operations are of different characteristics. They show a remarkable variation when compared with each other. The variations are judged by the degree of smoothness. A surface produced by super finishing is the smoothest while that by planing is the roughest. In the assembly of two mating parts, it becomes absolutely necessary to describe the surface finish in quantitative terms, which is the measure of micro-irregularities of the surface and expressed in microns.

1.5 Classification of Rough surfaces :

The surface roughness encountered in practice varies in their shape, size, distribution and arrangement, micro-scopical surface property, characteristics behavior with flow etc. For convenience they are classified as follows.

The roughness formed by sand particles or stone chips is called sand roughness. Nikurades described the sand roughness from technical point of view. The average absolute protrusion height of the roughness elements or the relative roughness heights with respect to some significant length are used to describe such roughness.

Rib roughnesses are employed by putting rectangular or cylindrical ribs on the surface transverse to the flow direction. Depending on the

ratio of the height of the roughness ribs and pitch, such roughness can be divided into D-type and K-type roughness. When the error in the origin is proportional to the height of the roughness elements then the roughness is called K-type or sand grain roughness. For a D-type roughness the error in origin is a linear function of the distance in the downstream direction. For specific engineering purposes the roughness elements for different geometrical shape are sometimes used, these are defined by their characteristic length. Another type of roughness termed as "tuft roughness" are also sometimes encountered. The examples of these types of roughness are grassy lands, green bushes, cornfields, and green mosses grown in the ship hull. The behavior of these types of roughness varies with the flow velocity and hence their analysis becomes complicated. The tuft roughness elements may show sticking character due to capillary action of narrow space present in between the fibers.

Different types of roughness can again be divided into two types, depending on how the surface roughness change is brought about. If the crest of the roughness elements lie above the preceding smooth surface, it is termed as upstanding surface roughness and if the crests lie below the smooth surface it is termed as the depressed type surface roughness.

The surface roughness of all type can again be expressed in terms of “equivalent sand grain roughness” as proposed by Nikuradse.

1.6 Objectives of The Study :

The study of the heat transfer due to circular wall jet is important due to its numerous practical engineering applications. In previous significant amount of work have been done on heat transfer due to wall jet of air on flat smooth or modified surfaces. In the literature no remarkable work is found related to distribution of pressure and heat transfer over flat rough surfaces. This is one of the prime interest behind the present investigation. The objectives of the present investigation are as follows :

- a) Determination of the pressure distribution over flat rough surfaces at various Reynolds numbers, Re and roughness, ϵ .
- b) Determination of local Nusselt numbers over flat rough surfaces at different Reynolds numbers, Re and roughness, ϵ .
- c) To develop a correlation for average Nusselt number in terms of Reynolds number and roughness of the surface.

CHAPTER – II

LITERATURE REVIEW



2.1. General :

The body of wall jet literature is large. Most early works were concentrated on wall jets on smooth flat surfaces. Wall jet on smooth and rough surfaces have been investigated in the present investigation.

G. E. Myers, J. J. Schaur, R. H. Eustis [1], observed that wall jet heat transfer differs from the common flat plate case due to the dissimilarities in the fluid mechanics between the two problem. The jet mixing in the wall jet, which causes the maximum velocity of decay, is not present in the flat plate. In this investigation, the wall jets with a step wall temperature distribution and thus allows extension to arbitrary heating condition. In this investigation experimental data have been presented describing the heat transfer aspects of two dimensional wall jet. It was found that the both temperature profiles and the relationship between the thermodynamic and the hydrodynamics properties of wall jets differ from the ordinary flat plate case. Near the start of heating, where the thermal effects are confined to a wall dominated region, the difference between the wall jet and the flat plate cannot be seen as the distance increases, both temperature profiles approach their corresponding velocity profiles.

Zerbe and Selna [2], were the only one to investigate a true wall jet. In their work the initial jet temperature was greater than the ambient. Jakob, Rose and Spielman [3] and Bergh et. al. [4], each have discussed the heated jet but also introduce another variable by having the jet parallel to the flat surface but not touching it.

Recently, Eckert et. al. [5], Seban [6] and Seban and Back [7], have discussed the case where the jet fluid is injected tangentially between a flat surface and a free-stream flowing over the surface. In each of these the injection of air was heated above the free-stream temperature.

R. A. Bajura and Albin A Szewczyk [8], made an experimental investigation of a two-dimensional wall jet at low Reynolds numbers with small natural disturbances in the jet. The main characteristics of the laminar regime are in agreement with theoretical results. The stability of the flow was studied for the Reynolds number ranging from 270 to 770.

H. Miyazaki and E. Silberman [9], analyzed theoretically the two dimensional laminar jets issuing from a nozzle of half width, which terminates at height above a flat plate normal to the jet.

A. J. Hogg et. al. [10], have been investigated and presented a new scaling law for the spatial variation of the mean velocity and lateral extent of a two-dimensional turbulent wall jet, flowing over a fixed

rough boundary. These scaling are analogous to those for the flow of a wall jet over a smooth boundary. They reveal that the characteristics of the jet depend weakly upon the roughness length associated with the boundary.

These laws are used in the development of an analytical framework to model the progressive erosion of an initially flat bed of grains by a turbulent jet. The grains are eroded if the shear stress, exerted on the grains at the surface of the bed, exceeds a critical value, which is a function of the physical characteristics of the grains. After the wall jet has been flowing for a sufficiently long period, the boundary attains a steady state, in which the mobilizing forces associated with the jet are insufficient to further erode the boundary.

Sato, Y, et. al. [11], investigated experimentally and numerically the interaction between dispersed particles and fluid turbulence for a vertical down-flow turbulent wall jet embedded in a uniform stream. Modifications of the mean fluid velocity by the particles induced reduction in the Reynolds stress, which alters the turbulence production. Turbulence modification by particles, with Stokes number of order of unity, is due primarily to the extra dissipation, which is a function of particle mean concentration and fluid turbulence in the fully developed region.

F. J. Higuera [12], has been studied numerically and analytically the coupling of the temperature and velocity fields by buoyancy in a laminar two-dimensional plane or circular wall jet over a finite length horizontal plate in the asymptotic limit of infinite Reynolds number. Two configurations are considered leading to cold layer of fluid over the plate, namely an ambient temperature jet over a cooled plate and a cold jet over an insulated plate. In both cases buoyancy generates an adverse pressure gradient that may separate the flow, if the Froude number is sufficiently small and always makes the solution everywhere over the plate dependent on the conditions at the downstream boundary. A separate analysis is carried out for very large Prandtl numbers showing that the recalculation bubble is then much shorter than the plate, also in agreement with the numerical results.

M. E. Stern et. al. [13], observed the spatial evolution of the two-dimensional turbulent flow from a source on the vertical wall of a shallow layer of rapidly rotating fluid which is strikingly different from the non-rotation three-dimensional counterpart, insofar as the instability eddies generated in the former case, cause the flow to separate completely from the wall at a finite downstream distance. In seeking an explanation of this, they first compute the temporal evolution of two-dimensional finite-amplitude waves on an unstable

laminar jet using finite difference calculation at large Reynolds number. This yields a dipolar vorticity pattern, which propagates normal to the wall, while leaving some of the near wall vorticity (negative) of the basic flow behind.

M. D. Zhou et. al. [14], measured three components of velocity fluctuation in a plane turbulent wall jet, which was modulated periodically by a sinusoidal pressure fluctuation in its settling chamber. The experiment was carried out in a closed-loop wind tunnel in the absence of an external stream at Reynolds number $Re_j = \frac{U_j b}{\bar{\nu}} = 6900$ and Strouhal number $St_j = \frac{fb}{U_j} = 9.5 \times 10^{-3}$, where b is the width of the slot from which the jet emerges at an efflux velocity U_j . A detailed comparison is provided with similar measurements made in a natural, unexcited turbulent wall jet. One of the purposes of this experiment was to establish the kinetic energy transfers, which take place in the wall jet under controlled perturbations.

D. Roy and S. R. Bhattacharya [15], investigated trough experiments the flows past a flat plate having different degrees of roughness. Special thrust has been imposed on the study of the change of coefficient of friction with the change of surface roughness.

V.Kuppu Rao [16], investigated and found many practical applications in the process of mass transfer from saturated porous surfaces exposed

to turbulent air streams. In many cases, the air stream will be in the form of wall jet over the porous surface.

G. P. Hammond [17], investigated and established an analytical expression for the complete velocity profile of a plane turbulent wall jet in stagnant surroundings is obtained by coupling Spalding's single formula for the inner layer with a sine function for the wake component.

Gardon and Akfirat [18], investigated the effect of turbulence on local heat transfer coefficient of impinging jets. They concluded that the heat transfer characteristics of impinging jets couldn't be explained in terms of velocity and position dependent boundary layer alone, but by accounting for the influence of turbulence. They later appeared to be uniquely dependent on the jet Reynolds number.

Goldstein et al. [19], experimentally investigated the heat transfer between a single circular air jet impinging on a heated flat plate that is 0.2405m wide and 0.107m long. In these high Reynolds number experiments ($6.2 \times 10^4 \leq Re \leq 1.24 \times 10^5$), the maximum stagnation Nusselt number (at $R=0$) occurred at $H \sim 8$, which is slightly higher than earlier values, $H \approx 6-7$, by Gardon and $H \sim 6$ by Tataoka.

Jambunathan et al. [20], made a detailed survey on the impingement cooling of a single air jet. They concluded that the simplest

correlation's for local convective heat transfer co-efficient is a function of the Reynolds number, $\frac{h}{d}$, $\frac{r}{d}$, and the Prandtl number.

Bouchez and Goldstien [21], investigated the impingement cooling of a circular jet with a cross flow or without a cross flow. It was found that as the jet-to-cross flow mass flux ratio decreases within a moderate range, the stagnation point will be deflected by the cross flow; consequently the stagnation point moves down stream. As the jet-to-cross mass flux ratio increases a recalculation and mixing zone was visualized. In the experiment the surface heat flux was in the range of 320-1200 W/m² and the jet spacing to-diameter ratio was arranged to be 6 and 12 respectively, since the surface heat flux is low and the jet spacing to-diameter ratio is high. The convective heat transfer co-efficient was found to be almost irrelevant to the surface heat flux.

Sparrow et al. [22], investigated the heat transfer of a vertical confined impinging circular jet with a cross-flow. The velocity of the cross-flow was fixed at 12 m/sec and the jet mean velocity was varied. It was found that the convective heat transfer coefficient with jet impingement could be ten times higher than that without an impinging jet. In the result the convective heat transfer coefficient was represented as a function of the jet to cross flow mass flux ratio, the location and the jet spacing to diameter ratio. For a mass flux ratio

more than eight, an optimum jet spacing-to-diameter ratio was clearly observed. The optimum ratio corresponds to a peak value of the convective heat transfer coefficient descends. Alternatively, as the jet spacing-to-diameter ratio is greater than the optimum value, the peak convective heat transfer coefficient also decreases due to a strong mixing effect.

The heat transfer of an unconfined jet impinging on a flat surface with low Reynolds number, an nozzle-to-surface spacing to jet diameter ratio was investigated by several investigators.

Huang and ElGank [23], investigated the heat transfer of an unconfined jet impinging on a flat plate with low Reynolds number and nozzle-to-surface spacing to jet diameter ratio by them. In this work the average Nusselt number was found to be proportional to $Re^{0.76}$. The measurement of the heat transfer of an unconfined impinging jet with the nozzle-to-surface spacing to jet diameter ratio less than 1.0 was performed by Lytle and Webb [43]. For a nozzle-to-surface spacing less than 0.25 times the jet diameter the effect of fluid acceleration between the nozzle wall and impingement surface was seen; this results in a clear observation of the secondary maxima in the Nusselt number.

Huber and Vistanta [24], investigated the effect of jet to sheet spacing on convective heat transfer to a confined impinging jet array. A thermochromatic liquid crystal technique was used to visualize and measure the isotherms on the impingement plate. They found that, for a high separation distance between the jet and impingement plate, the adjacent jet interference before impingement will cause significant degradation of the convective heat transfer coefficient. The effect of a spent air arrangement on the heat transfer was also investigated. It was found that the spent air results in a heat transfer enhancement by minimizing adjacent jet interference in the wall jet region.

The diameter dependency on the Nusselt number for a jet impinging on an isothermal plate was investigated by Hollworth and Gero [25], they investigated that, for the cases with values of $\frac{h}{d}$ greater than 10, the jet diameter has no effect on the Nusselt number. Due to the limitation of the measurement, this experiment did not verify this point for cases with a lower value of $\frac{h}{d}$. Stevens and Webb [26] investigated the local heat transfer coefficient for a free liquid jet impinging normally on a uniform heat flux surface. The ratio of mean jet velocity to jet diameter was proposed, in the correlation, to vanish the nozzle size dependency. The local heat transfer from a small heat source to a normally impinging, confined and submerged liquid jet was experimentally

investigated by Garimella and Rice [27], they investigated that the nozzle-to-heat source spacing, jet Reynolds number and nozzle diameter were explored as variables. The result indicates that at the stagnation point, for a given Reynolds number and nozzle-to-heat source spacing, the smaller nozzle produces a lower Nusselt number. The correlation for the stagnation point and area-average heat transfer coefficient were expressed in terms of jet Reynolds number, fluid Prandtl number, nozzle-to-heat source spacing and nozzle aspect ratio.

Jung-Yang San, Chih-Hao Huang and Ming-Hong Shu [28], investigated the local Nusselt number of a confined circular air jet vertically impinging on a flat plate. The aspect ratio of the jet orifice was 1.0. Four different jet hole diameters, namely 3.0, 4.0, 6.0 and 9.0 mm were considered individually. The Reynolds number, the surface heating width and the surface heat flux, on the heated area were the variables in the measurement. It was intended to realize the effect of the jet hole diameter on the heat transfer of a confined jet impingement, for various operating conditions.

A few more investigations of jet impingement combined with extended surfaces have reported generally promising results.

Ali Khan et al. [29], positioned a punched plate with circular holes upstream of a heated surface.

Hrycak [30] studied heat transfer for a jet impinging on a smooth plate modified with spike and concentric ring proturbulence.

Obot and Trabold [31], investigated arrays of jets impinging on surfaces having repeated square ribs with transverse flow of the spent air.

Hensen and Webb [32], performed an experiment to characterize heat transfer to a normally impinging air jet from surfaces modified with arrays of fin-type extension. Heat transfer enhancement for six-fin geometries was evaluated by comparison with result for a smooth, flat surface. Average Nusselt number and overall system effectiveness is reported as function of fin type, jet Reynolds number, and nozzle-to-surface spacing for two nozzle diameters. Enhancement of the absolute rate of heat transfer, as compared to the smooth surface, was demonstrated by a factor ranging from 1.5 to 4.5. The system effectiveness as a function of Re exhibited strong fin type dependence due to significant variations in the total surface area and average Nusselt number. The fin type dependence of Nu as a function of Re was found to be a result of variations in the turbulence level, fluid velocity, and the percentage of total surface area exposed to normal, oblique, and parallel flow. The average Nusselt number correlated well in the form, $Nu = C \cdot Re^m$. For the modified surfaces, the system

effectiveness decreased monotonically with increasing in contrast to the smooth surface behavior. Some investigators have observed pressure distribution over surfaces by impinging jet.

Hossain. K.A. and Arora. R.C. [33], described that impinging jet behaves essentially like a free jet ahead of stagnation point. The pressure does not remain constant. Pressure increases as the flow approaches the stagnation region. In the stagnation region, the center line velocity decreases to a zero value and pressure approaches to the maximum at the stagnation point.

Ali. M.A.T., Hasan. A and Islam. M.T. [34], described that, at the beginning of the rough surface the wall static pressure suddenly dropped from its smooth wall pressure gradient. Wall shear stress was found to increase more or less proportionately with the roughness height. At smooth rough junction, the roughness height caused the near wall flow to deflect upwards resulting in the production of secondary current which died out quickly away from the wall.

Md. Nurul Islam [35], investigated the pressure distribution and the local and average Nusselt number due to impinging of a circular air jet over uniformly heated rough flat surfaces.

Very recently, jet impinging on arrays of blocks mounted on otherwise flat surface (simulated electronic packages) has attracted considerable attention. [36-37].

A number of investigators have observed that the relatively high heat transfer characteristics of impinging jets are related to high turbulence levels in the fluid flow as found in the references 38, 39, 40, 41 & 42. A variety of turbulence promoting scheme have been used to enhance jet impingement heat transfer with varying degree of success.

The present study serves to investigate the pressure distribution over rough surfaces at various Reynolds numbers Re and roughness, ϵ of the surface. The present study investigates the local Nusselt numbers over rough surfaces and develops a correlation for average and maximum Nusselts numbers relating jet exit Reynolds numbers and roughness of the surfaces.



CHAPTER – III

METHODOLOGY

3.1 Calculation of Surface Roughness :

The roughness of the surface can be measured by the following methods :

1. Centerline Average Method (C.L.A. method)

2. Root Mean Square Method (R.M.S. method)

3.1.1 Center Line Average Method :

The centerline average method is defined as the average value of the ordinates between the surface and the mean line, measured on both sides of it. The surface finish is measured in terms of C.L.A. value and it is denoted by R_a . Mathematically, C.L.A. or

$$R_a \text{ (in microns)} = \frac{h_1 + h_2 + h_3 + \dots + h_n}{n}$$

Where, $h_1, h_2, h_3, \dots, h_n$, are the ordinates measured on both sides of the mean line and 1, 2, 3, ..., n, are the number of ordinates. This method is conventionally used to measure or calculate the surface roughness.

3.1.2 Root Mean Square Method :

The root mean square method is defined as the square root of the arithmetic mean of the square of the ordinates. Mathematically,

$$\text{R.M.S.} = \sqrt{\frac{h_1^2 + h_2^2 + h_3^2 + \dots + h_n^2}{n}} \quad \text{in microns}$$

Where, $h_1, h_2, h_3, \dots, h_n$ are the ordinates measured on both sides of the mean line and n is the number of ordinates.

3.2. Experimental Set-Up :

The experimental set-up is shown in Figure 3.1. The different components of the experimental setup are as follows.

- 1) Air jet and pressure measuring system.
- 2) Jet support frame.
- 3) Heater and test surface arrangement.
- 4) Temperature measuring system.

3.2.1 Air jet and Pressure measuring arrangement :

The air jet was issued from a circular copper tube of inside diameter 6.2mm. The length of the tube was 320 mm, which was sufficiently larger than hydraulic diameter (120 ID) to ensure fully developed flow.

The jet system and its different views are shown in Figure 3.1.

The jet arrangement consisted of an air blower (1.5 hp), a variac, a filter cum settling chamber, a flow straightner, a Pitot tube (Niddle), an inclined manometer for air, a converging nozzle of diameter 6.2 mm.

3.2.2 Jet support arrangement :

The jet support frame was used to adjust the elevation of the jet exit from the heated impingement surface and to maintain the jet in vertical position.

3.2.3. Heater Assembly Including Test Surfaces :

The heated plate was of 0.195mm thick (34 gage) M.S. sheet, measuring 140mm x 140mm ($k=54\text{w/m.k}$). The sheet was laid perfectly flat on a 25.4mm thick Bakelite slab ($k=0.23\text{ w/m.k}$) over laid on 25.4mm thick cork sheet ($k=0.42\text{ w/m.k}$) and on a temper glass sheet and the perimeter of the M.S. sheet and Bakelite was insulated by the cork sheet. The M.S. sheet was heated uniformly using two plate type heaters of 150W, 220V each. Heaters were connected with 220 volt A. C. supply in series as shown in Figure 3.2 .

Investigations were performed on 5 (five) test surfaces. One of them was smooth and others were of different roughness. The surfaces artificially roughened by scribers of various sizes in random manner. Dial gauge indicator is used to measure the surface roughness and

roughness was calculated by using the centerlines Average method (C.L.A method).

3.2.4. Temperature measuring arrangement :

Digital temperature recorders recorded surface temperatures of the sheets. These recorders were connected with sheets as shown in Figure 3.2. Thermocouple leads were of K-type (Cromel-Alumel) couple. The thermocouple leads were inserted through the upper surface of the Bakelite slab and the ends of the thermocouple wire were soldered to maintain in a good contact with the underside of the heated sheets during the experiments.

3.3 Experimental Technique :

Throughout the experiments the jet was centered along the surface, airflow was adjusted by rotating the knob of the variac. Then velocity of the airflow was measured by Pitot tube and manometer (by which velocity of air and jet Reynolds number was calculated). When the flow became stable and fully developed the manometric head of the fluid is measured and the jet exit Reynolds number is calculated. At this position, pressure distribution over flat surface due to jet of air was recorded. At this stage the blower is stopped and the heater is turned on to heat the surface and after attaining the steady state temperature, the temperature of the surface is recorded which is T_w . Then the flow

of jet is started and after attaining steady state temperature, again the temperature, T at different locations along the length of the surface were recorded. At the same time the jet temperature of T_j also was recorded. Surface temperature before airflow, air temperature at nozzle exit, ambient temperature and surface temperatures (after flow of fluid) were recorded by digital temperature recorders.

The procedure was followed for each surface such as, smooth, $\epsilon=0.01371$, $\epsilon=0.01435$, $\epsilon=0.01581$ and $\epsilon=0.01613$ and for Reynolds numbers are 8799, 10777, 16849 and 18804.

3.4 Error Analysis :

The uncertainty in the measurement can be separated into two parts. The first is from the mass flowrate; the second is from the convective heat transfer coefficient. The former is due to the inaccuracy of the turbine flowmeter. According to the manufacturer's supplied data 1% error on the measurement is assured. The inaccuracy of the latter is attributed to the following reasons.

3.4.1 Heat flux error :

- * Radiation loss, 3.1%;
- * Non-uniformity of the heating plate, less than 4.4%;
- * Lateral solid heat conduction, 2.0%;
- * Heat loss through insulation, 0.9%.

3.4.2 Temperature error :

* Inaccuracy due to thermocouple, $35 \pm 0.2^{\circ}\text{C}$.

In the experiment a high accuracy of the temperature measurement is demanded. In the evaluation of the convective heat transfer coefficient only the difference of the adiabatic wall temperature and heated wall temperature is needed. In this work the same thermocouple is used to measure the two temperatures, thus the inaccuracy of the temperature measurement is reduced. Neglecting the error in the temperature measurement the uncertainty in Nusselt number of this experiment is 5.81%.

Table 1 : Specification of the Instruments

NAME	MANUFACTURE	SPECIFICAION
1. Air Blower	Alladays & Onion Ltd. Bermingham.	hp.- 1.5, Rpm 5200. Amp-1.2, Volts-220/250. 50Hz.
2. Variac	The Electric Apparatus Ltd. England.	Volts-60/200, Ohm-500. Amp-45.
3. Pitot tube	A niddle of diameter 0.45 mm is used as pitot tube.	One way
4. Inclined manometer for air.	Airflow development Ltd. High Wycomb, G.B.	Range -0-2.5 kN/m ²
5. Plate type heater	Made in India.	150 W (2nos), 220 Volts.
6. Digital Temperature Recorder.	KKK-MC-03230240 Made in Taiwan.	0 ⁰ C-800 ⁰ C.

Table 2 : Nominal Experimental Condition

Name	Experimental Condition
1. Ambient temperature and pressure	30 ⁰ C; 101.325 kN/m ² .
2. Jet diameter	6.2mm.
3. Sheet specifications	140mm.x140mm.x0.195mm.
4. Reynolds number	8799,10777, 16849 & 18804.
5. Fluid	Air at 30 ⁰ C and of thermal conductivity is 0.026W/m. K.
6. Pitot tube	Niddle is used as pitot tube. Nozzle-to-Niddle inlet diameter ratio is 13.37.

CHAPTER – IV

RESULTS AND DISCUSSION

4.1 General :

In the present investigation the pressure distribution and heat transfer characteristics over smooth and rough surfaces due to circular wall jet was investigated. Experiments were performed for jet Reynolds number 8799, 10777, 16849 and 18804 for jet diameter of 6.2 mm. The surfaces were considered of smooth and relative roughnesses of 0.01371, 0.01435, 0.01581 and 0.01613.

4.2 Pressure Distribution :

The distribution of co-efficient of pressure over the surface of different roughnesses were plotted for different Reynolds number in Fig. 4.1.1 to Fig. 4.1.5. Also the distribution of co-efficient of pressure were plotted for different relative roughnesses in Fig. 4.1.6 to Fig. 4.1.9.

4.2.1. Effect of Reynolds number on Pressure distribution :

Figure 4.1.1, shows the distribution of co-efficient of pressure, C_p along the length of the smooth surface at various Reynolds number, Re . It was observed that the co-efficient of pressure decreases with the increase of Reynolds number and decreases along the length of the surface and becomes steady at $X = 13.0$, but showed maximum value at the starting point. Because agitation play roles in the laminar sub-

layer. The turbulence creates in the laminar sub-layer due to the protrusions of the rough surface, which is absent in smooth surface. If the Reynolds number increases the flow is separated from the surface. The decreasing rate of co-efficient of pressure is higher at lower Reynolds number. Figure 4.1.2 to 4.1.5 show the variation of co-efficient of pressure at different Reynolds number for various surface roughness. The similar trend was observed as for the smooth surface, but the starting point value as well as the values along the length of the surface is relatively lower. It was also observed that the co-efficient of pressure decreases with the increase of roughness of the surface.

4.2.2 Effect of Surface Roughness on pressure distribution :

Figure 4.1.6, shows the distribution of co-efficient of pressure along the length of the surface at jet exit Reynolds number $Re = 8799$. It was observed that the co-efficient of pressure decreases with the increase of relative roughness of the surfaces. The decreasing rate of co-efficient of pressure is higher at smooth surface and surface of lower relative roughness, but the curve becomes almost flat in nature at higher value of relative roughness surface. If the average height of the protrusions increases, the turbulence generated in the laminar sub-layer. As a result the flow is separated from the surface and mixed with the buffer layer. It was also observed that the starting value of co-efficient of pressure is

higher at smooth surface, but the starting value is decreasing with the increase of relative roughness of the surface.

Figure 4.1.7 to 4.1.9, show the variation of coefficient of pressure, C_p along the length of the surface X for different Reynolds number at smooth and rough surfaces. It was observed that the co-efficient of pressure decreases with the increase of surface roughness at a particular Reynolds number and also show that the decreasing rate is higher at lower value of Reynolds number.

4.3. Heat transfer characteristics :

The experiments were carried out to investigate the heat transfer characteristics over the surfaces of various roughness for different jet exit Reynolds numbers, Re . The measured local Nusselt number, Nu over the surfaces of different roughness and jet exit Reynolds number were plotted as shown in Fig. 4.1.10 to 4.1.18.

4.3.1. Effect of Reynolds number on heat transfer characteristics :

Figure 4.1.10, shows the distribution of local Nusselt number Nu along the length of the smooth surface at various Reynolds number Re . It was observed that the local Nusselt number increases with the increase of Reynolds number but decreases along the length of the surface and becomes steady at $X = 8$, but shows maximum value at the starting



point. Because of higher Reynolds number turbulence is generated in the laminar sub-layer, which than mixed in the buffer layer of the boundary layer. For higher Reynolds number the flow contains higher kinetic energy.

Figure 4.1.11 to 4.1.14, show the variation of local Nusselt number at different Reynolds number for various surface roughnesses of the plate. The similar trend was observed as for the smooth plate but the starting point value as well as the values along the length of the surface is relatively lower. It was also observed that the Nusselt number increases with the increase of roughness of the surfaces.

4.3.2 Effect of surface roughness on heat transfer characteristics :

Figure 4.1.15 shows the distribution of local Nusselt number Nu with relative roughness for jet exit Reynolds number $Re = 18804$. It is observed that the local Nusselt number decreases with the increase of length along the surface. Average height of protrusion increases with the increase of roughness of the surface. As a result the flow in the laminar sub-layer separated from the surface as well as turbulence is generated in the laminar sub-layer. The protrusions in the rough surface act as fins attached to the surface. Therefore, transfer of heat enhanced for rough surfaces. The maximum value of the local Nusselt

number was obtained at the starting point and the maximum value of local Nusselt number increases with the increase of relative roughness of the surface.

Figure 4.1.15 to 4.1.18, show the variation of local Nusselt number Nu at various surfaces for different Reynolds Number. It is observed that the local Nusselt number for smooth surface is lower than the rough surfaces for all Reynolds number and increases with the increase of surface roughness and also decreases with the decrease of jet exit Reynolds number.

4.4 Correlation for Average Nusselt number :

The experimental values of local Nusselt number, Nu were used to calculate the Average Nusselt number, \overline{Nu} based on the local temperature difference, as a function of radial distance, using the relation,

$$\overline{Nu} = \frac{\sum Nu_x \cdot x}{L} \quad [1]$$

The correlation for Average Nusselt number has been developed in terms of jet Reynolds number (Re), relative roughness (ϵ), but not applicable for smooth surface. The correlation is determined using the

least square curve fit method based on the experimental data. The present correlation for \overline{Nu} is as follows,

$$\overline{Nu} = 43Re^{0.25} \epsilon^{0.45} \quad [2]$$

However, as shown in Figure 4.2, the agreement of correlation was within $\pm 10\%$ accuracy of the experimental data covering the complete range of parameters.

CHAPTER – V

CONCLUSION

In this concluding chapter, the highlights of the findings of the present investigations have been presented. The scope of extension of the present research facility is also outlined with a view to acquire more knowledge from the same situation.

In light of the discussion of results the following conclusions were drawn as a consequence of present work.

5.1. Conclusion for pressure distribution :

Variation of pressure distribution due to wall jet over a surface depends on surface roughness, jet Reynolds number in the following manner.

1. Co-efficient of pressure decreases with the increase of jet Reynolds number and jet Reynolds number has significant effect on pressure distribution.
2. Co-efficient of pressure decreases with the increase of surface roughness.
3. Co-efficient of pressure is maximum at the initial point for all relative surface roughnesses and all jet exits Reynolds number within the range of parameters considered in the Experiment.

4. Co-efficient of pressure in smooth surface is higher than that of rough surface.
5. The decreasing rate of co-efficient of pressure is higher at smooth surface and surface of lower relative roughness.

5.2. Conclusion for Heat Transfer Characteristics :

Heat transfer characteristics due to circular wall jet over rough surfaces depend on relative surface roughness, ϵ jet Reynolds numbers, Re in the following manner.

1. Nusselt number increases with the increase of roughness of the surface.
2. Nusselt number increases with the increase of jet Reynolds number.
3. At starting point Nusselt number decreases with the increase of surface roughness.
4. Decreasing rate of local Nusselt number is higher at higher Reynolds number.
5. Nusselt number in smooth surface is lower than that of rough surface.
6. A correlation has been developed for calculating the average Nusselt number, \overline{Nu} within $\pm 10\%$ accuracy based on experimental data.

5.3. Scope of further work:

The following suggestions are put forward as an extension of the present investigation.

1. The same work can be repeated with more different size of rough surfaces and at higher jet Reynolds number.
2. The same experiment can be repeated by using the air jet.
3. The same experiment can be repeated by using the oblique jet.

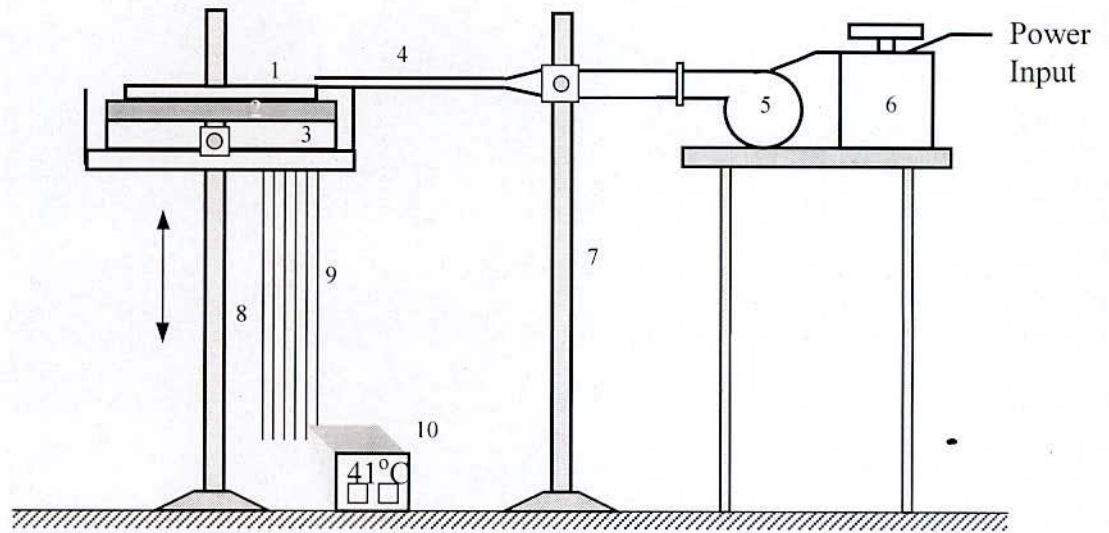


Figure 3.1 Schematic diagram of Experimental Setup

- | | |
|-----|----------------------|
| 1. | M.S. Sheet |
| 2. | Bakelite Sheet |
| 3. | Cork Sheet |
| 4. | Copper tube jet |
| 5. | Air blower |
| 6. | Variac |
| 7. | Blower Stand |
| 8. | Bakelite Sheet Stand |
| 9. | Thermocouple wire |
| 10. | Temperature Recorder |

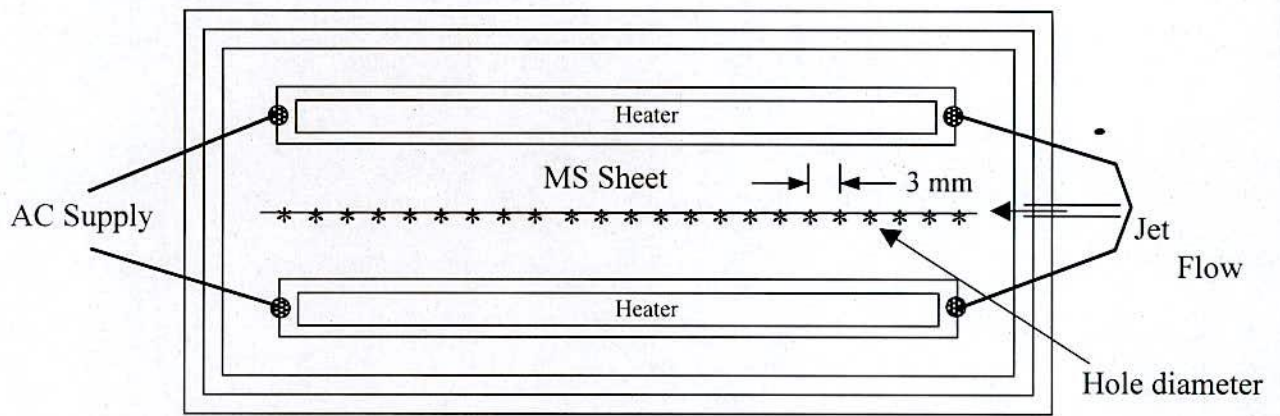


Figure No. 3.2 M.S. Sheet test section

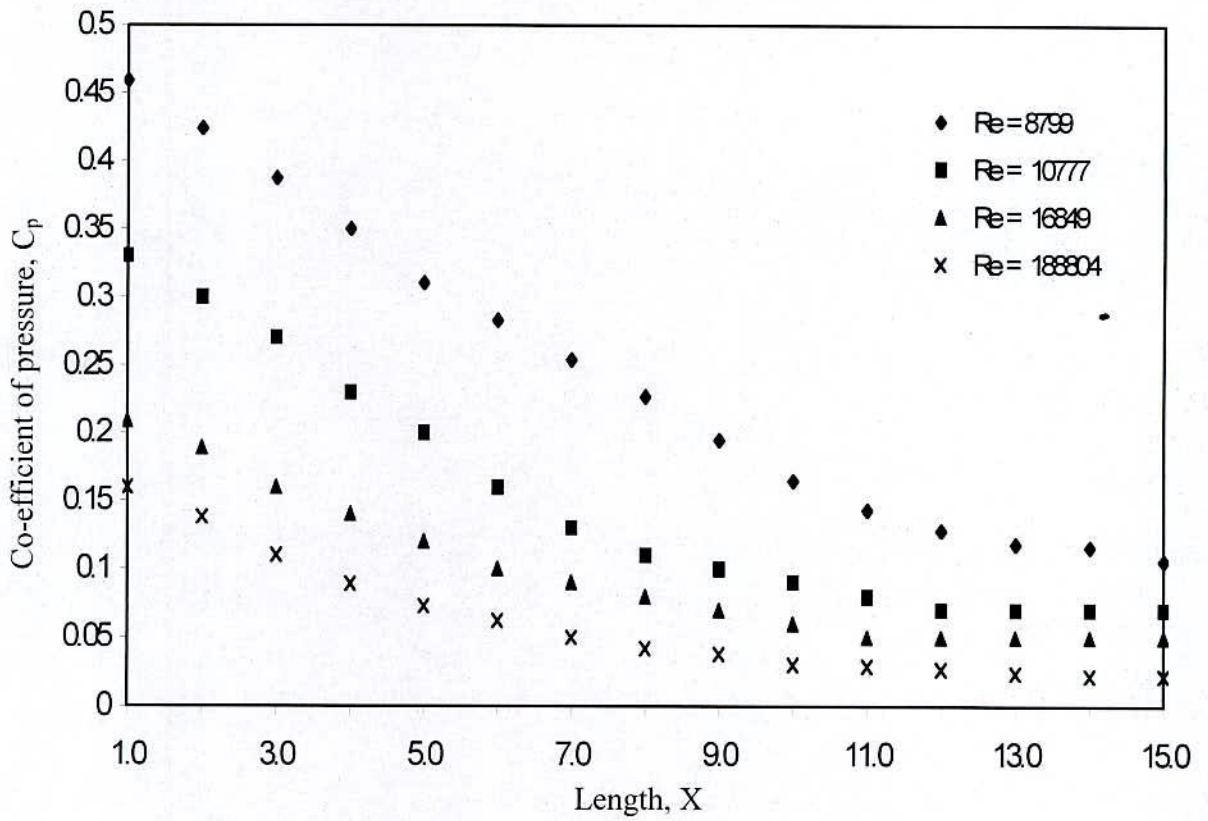


Figure 4.1.1 Distribution of co-efficient of pressure, C_p along the length of the smooth surface at various Reynolds numbers

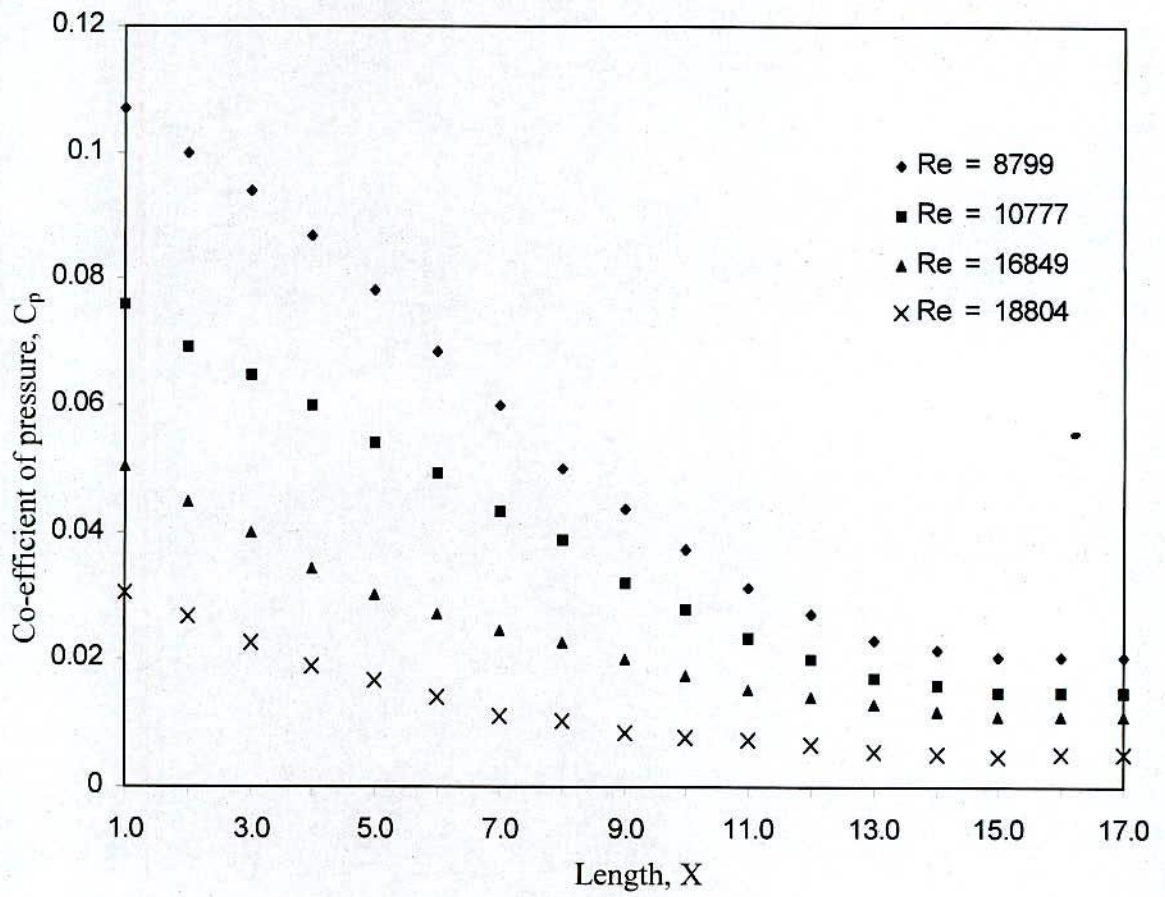


Figure 4.1.2. Distribution of co-efficient of pressure, C_p along the length of the surface roughness $\epsilon = 0.01371$ at various Reynolds number.

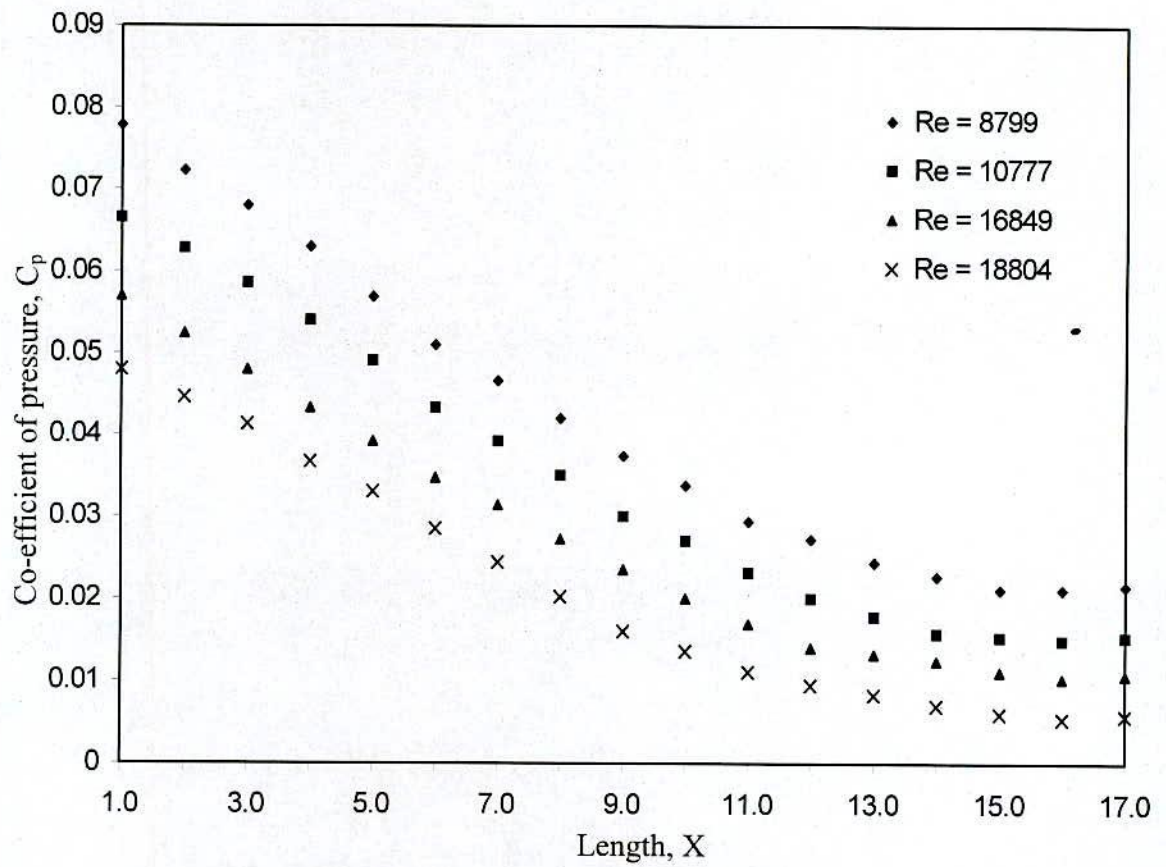


Figure. 4.1.3 Distribution of co-efficient of pressure, C_p along the length of the surface roughness $\epsilon = 0.01435$ at various Reynolds number.

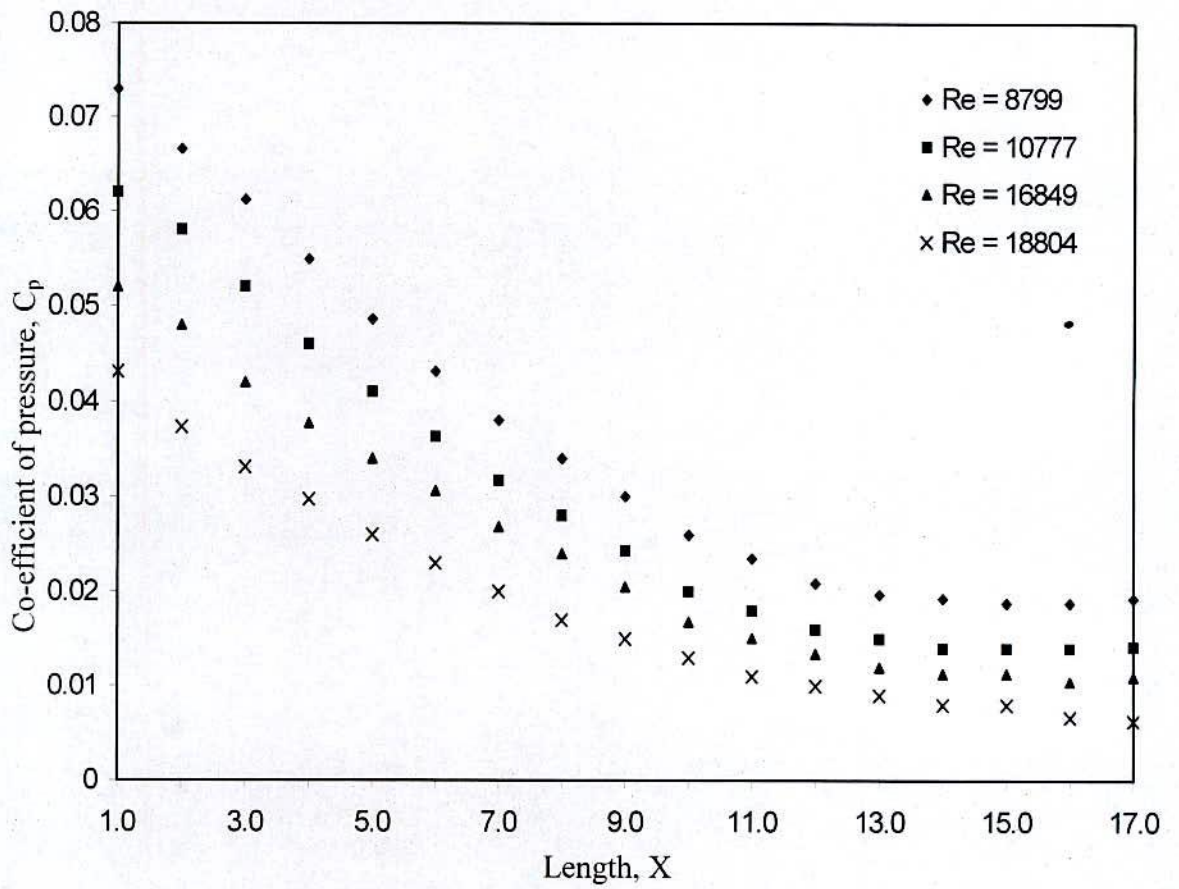


Figure 4.1.4. Distribution of co-efficient of pressure, C_p along the length of the surface roughness $\epsilon = 0.01581$ at various Reynolds number.

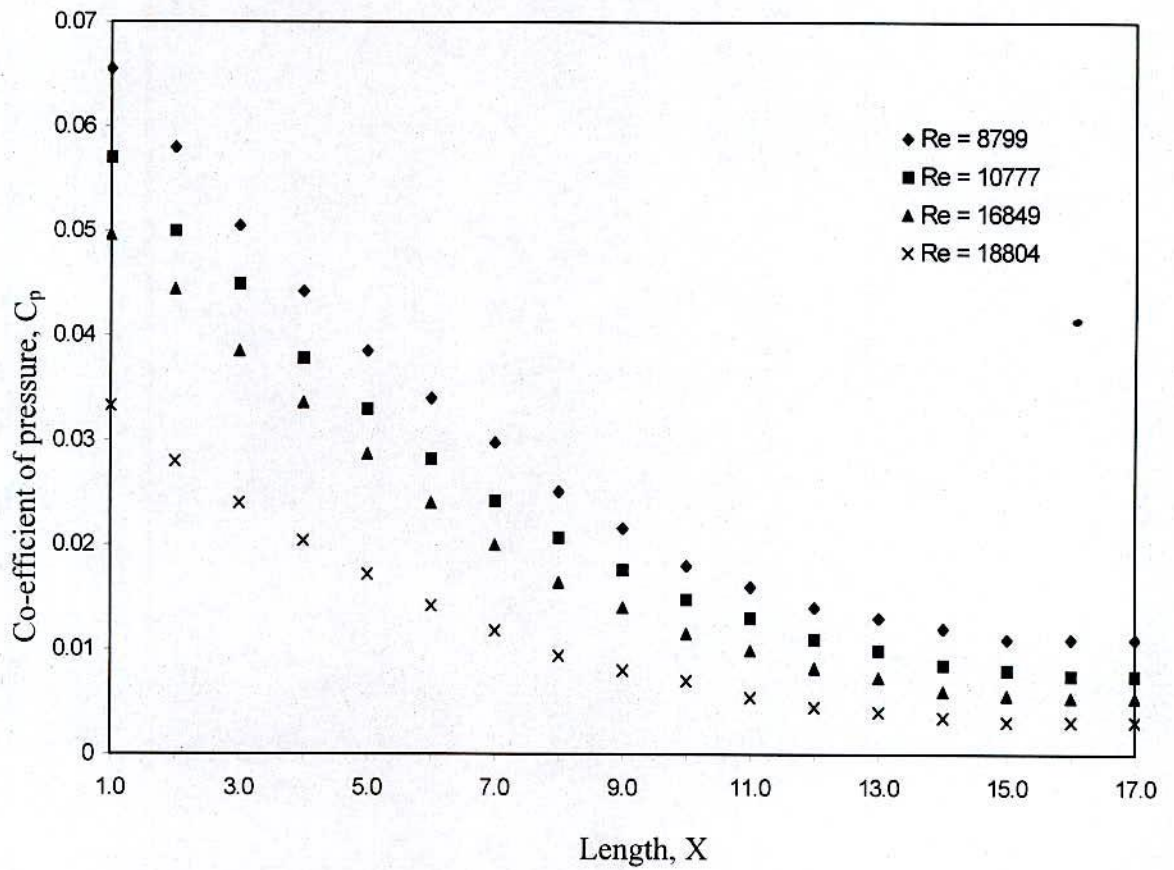


Figure 4.1.5 Distribution of co-efficient of pressure, C_p along the length of the surface roughness $\epsilon = 0.01613$ at various Reynolds number.

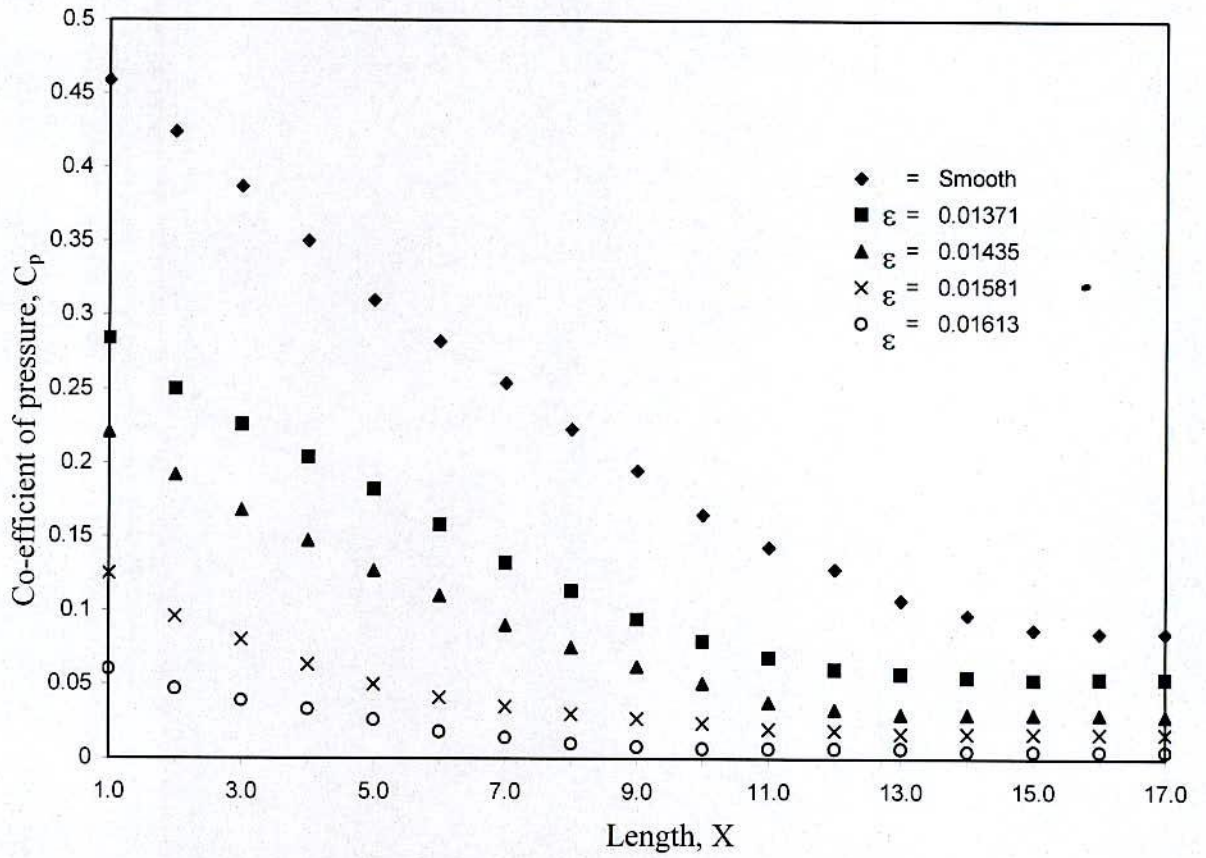


Figure 4.1.6. Distribution of co-efficient pressure C_p along the length of the surfaces at jet exit Reynolds number $Re = 8799$

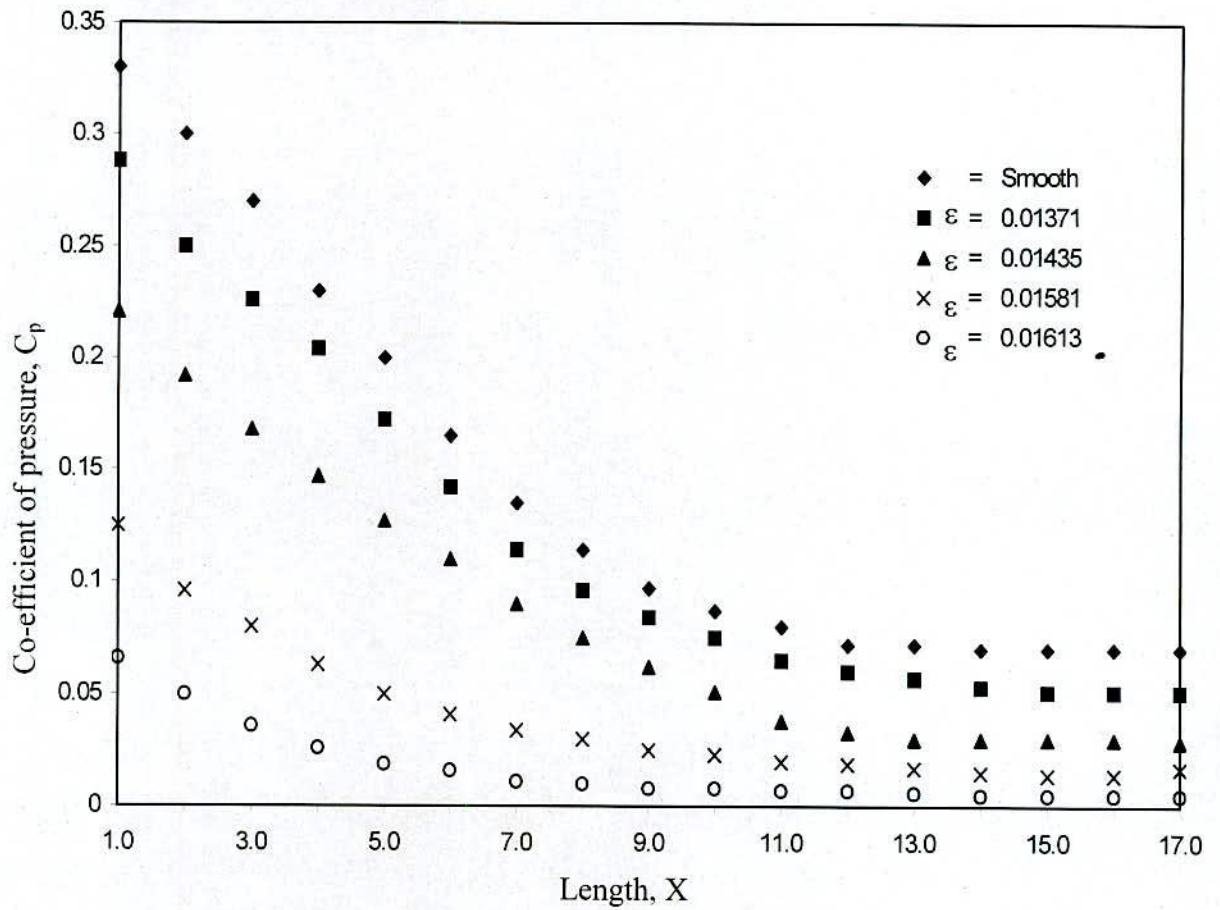


Figure 4.1.7. Distribution of co-efficient pressure C_p along the length of the surfaces at jet exit Reynolds number $Re = 10777$

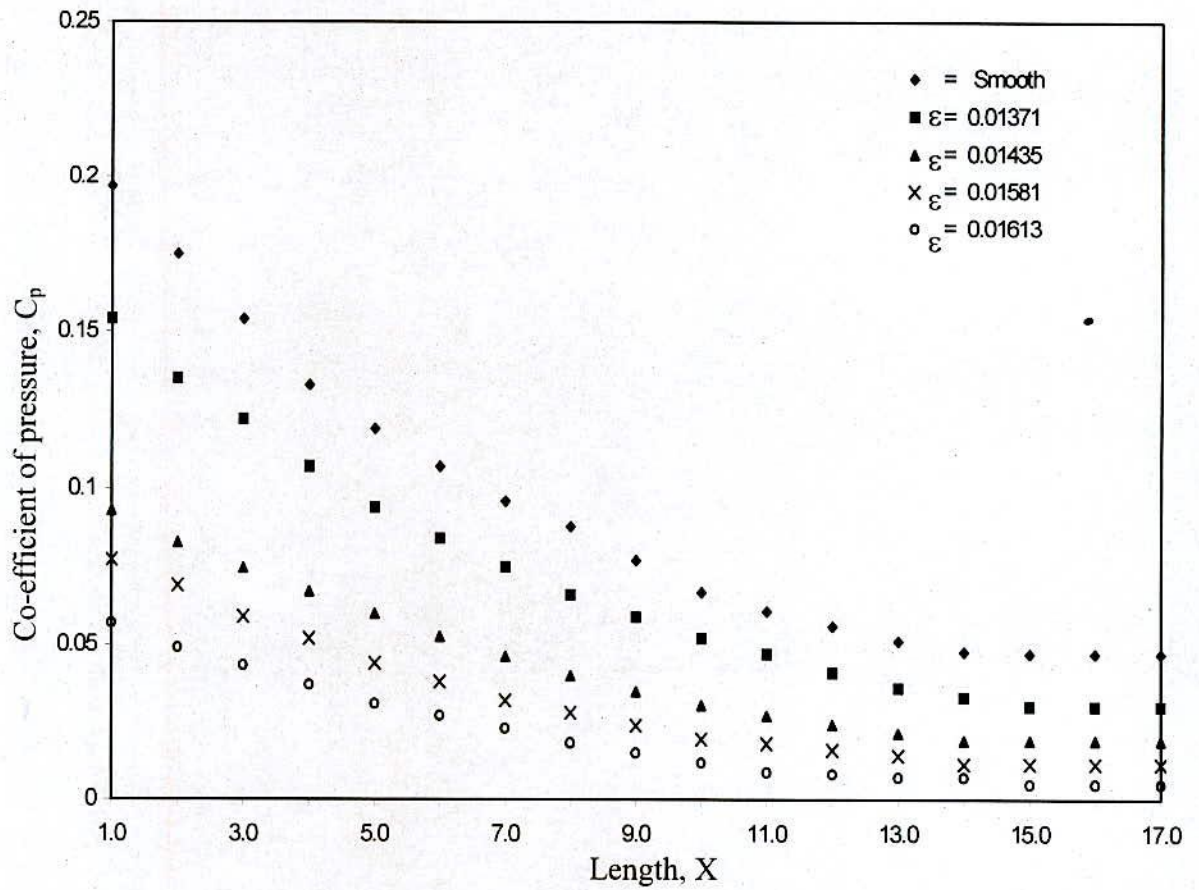


Figure 4.1.8. Distribution of co-efficient pressure C_p along the length of the surfaces at jet exit Reynolds number $Re = 16849$.

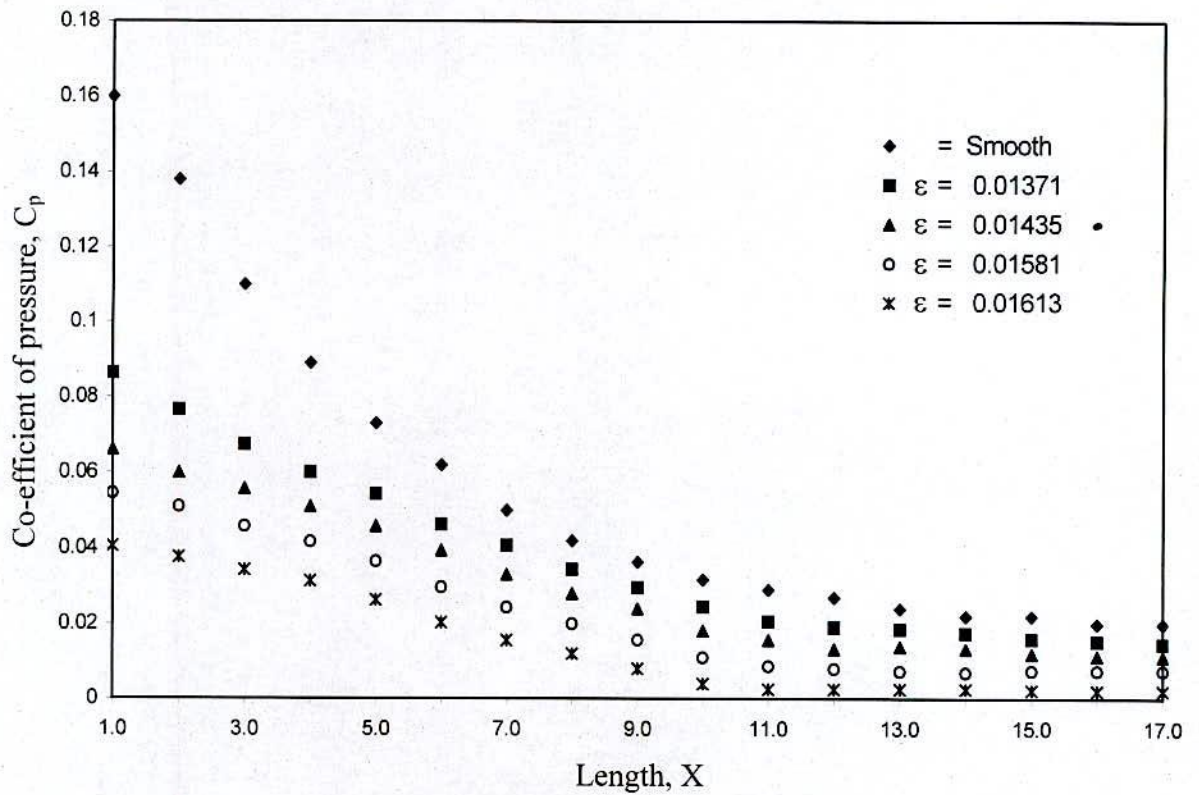


Figure 4.1.9. Distribution of co-efficient pressure C_p along the length of the surfaces at jet exit Reynolds number $Re = 188804$

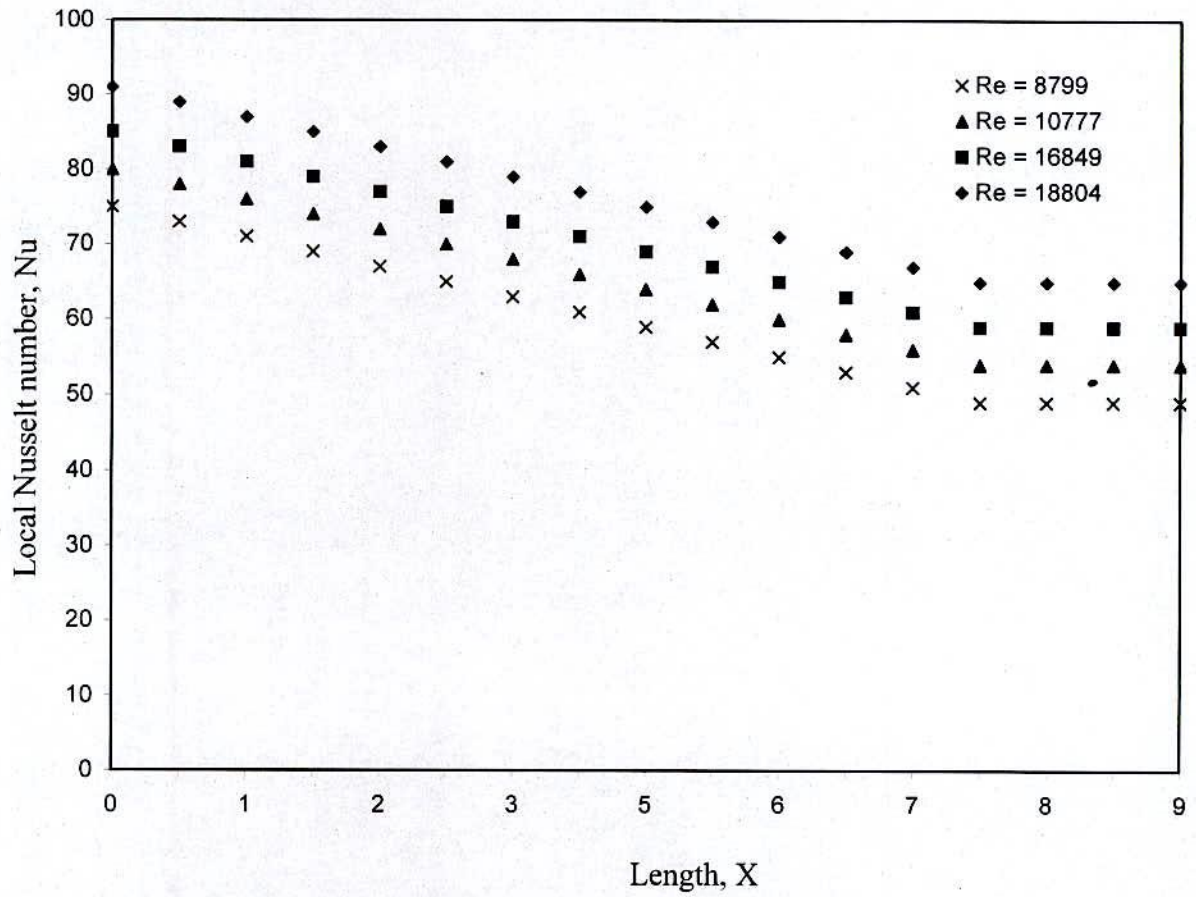


Figure 4.1.10. Distribution of local Nusselt number over a smooth surface at various jet exit Reynolds. number

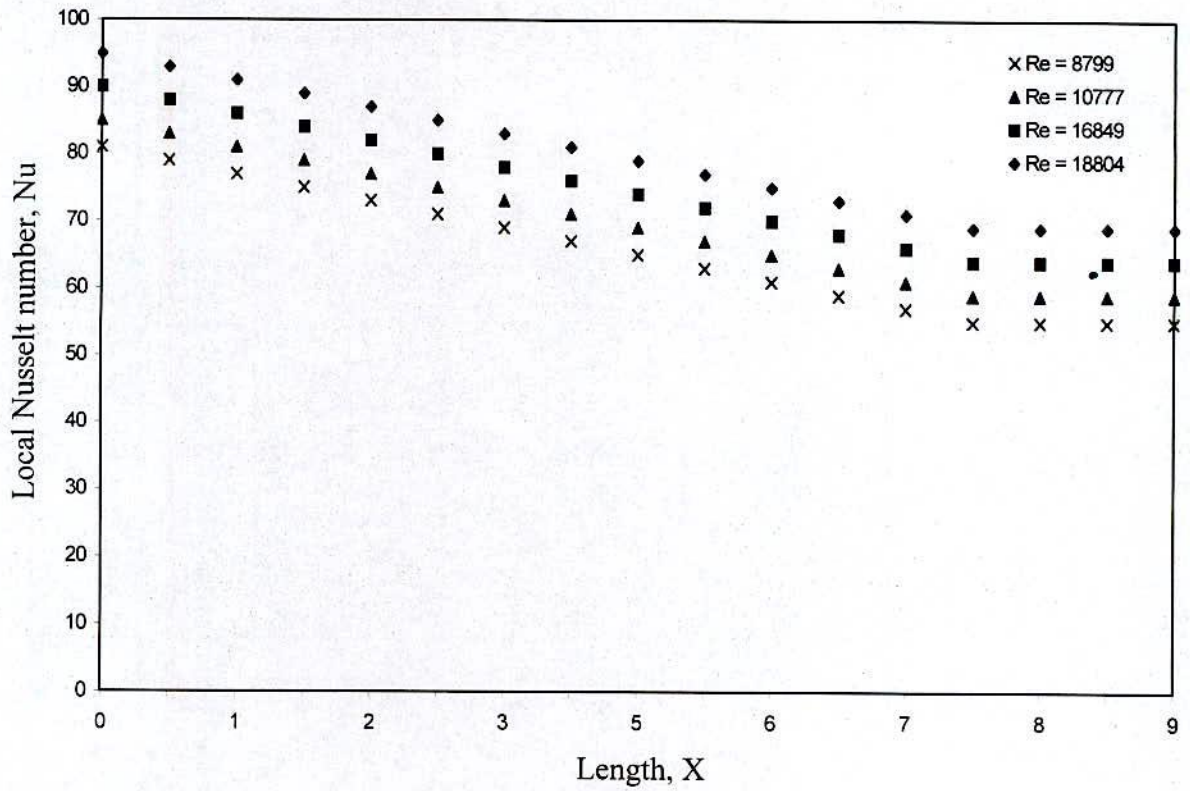


Figure 4.1.11. Distribution of local Nusselt number over the surface of roughness, $\epsilon = 0.01371$ at various jet exit Reynolds number.



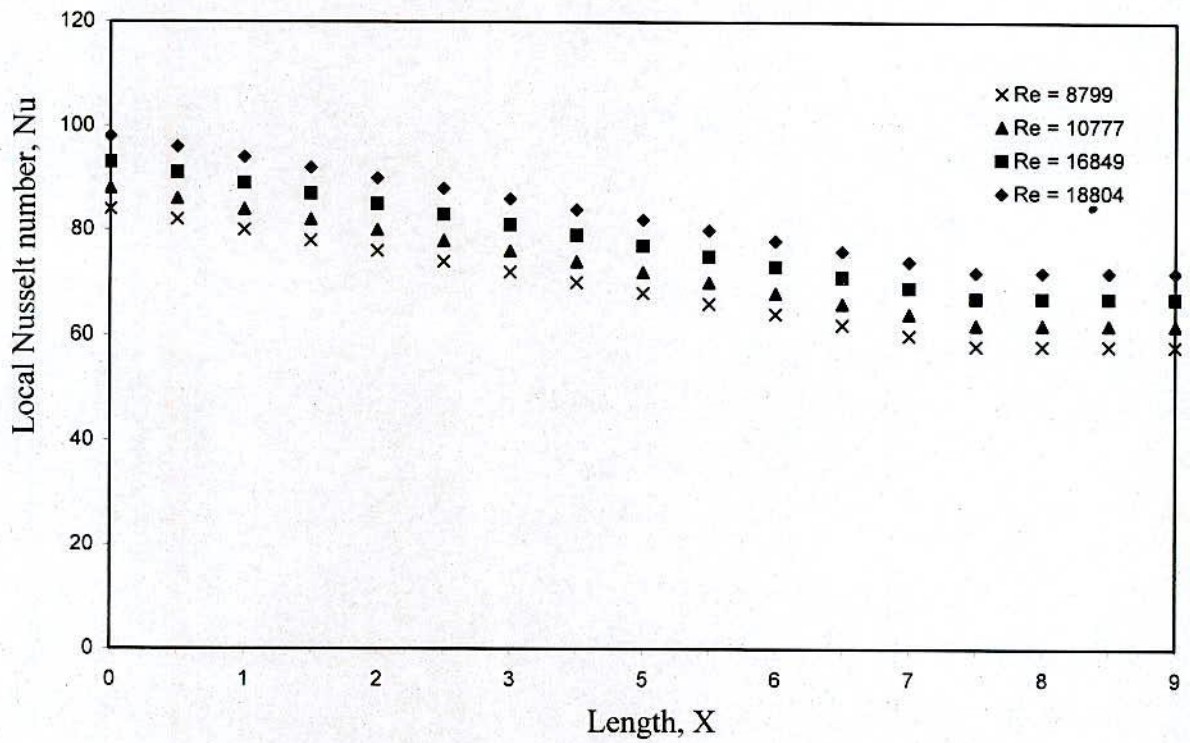


Figure 4.1.12. Distribution of local Nusselt Number over surface of roughness, $\epsilon = 0.01435$ at various jet exit Reynolds number.

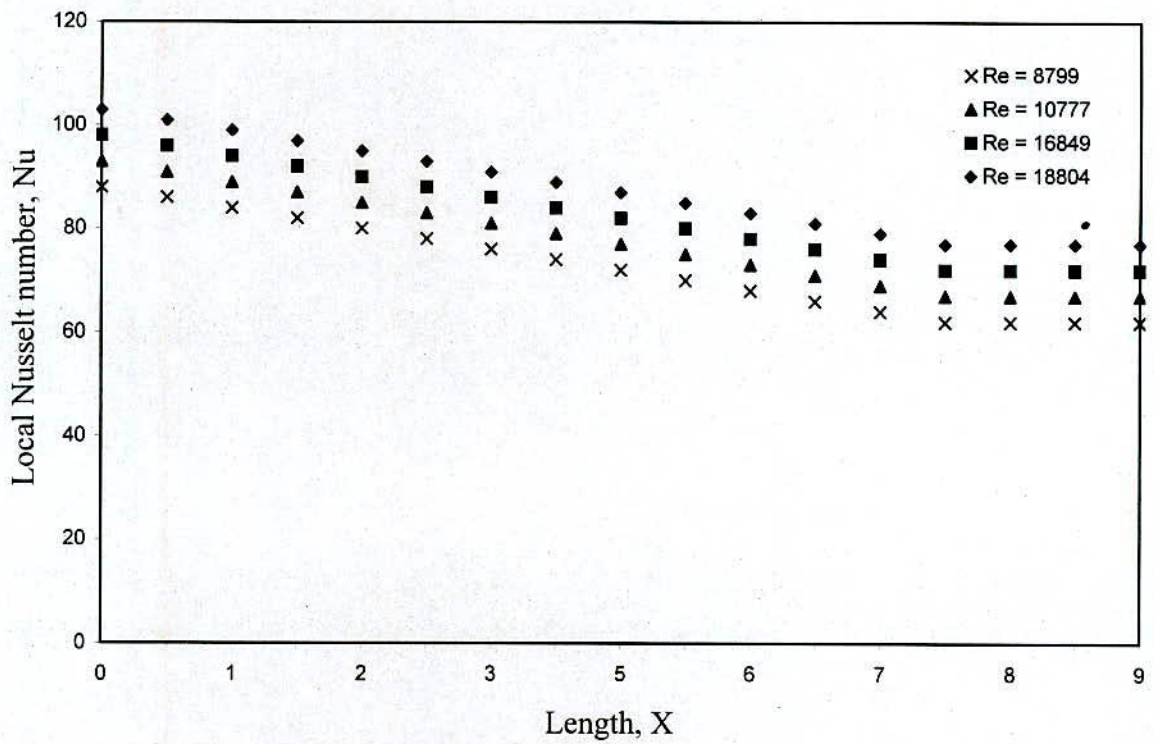


Figure 4.1.13. Distribution of local Nusselt number over the surface of roughness, $\epsilon = 0.01581$ jet exit various Reynolds number.

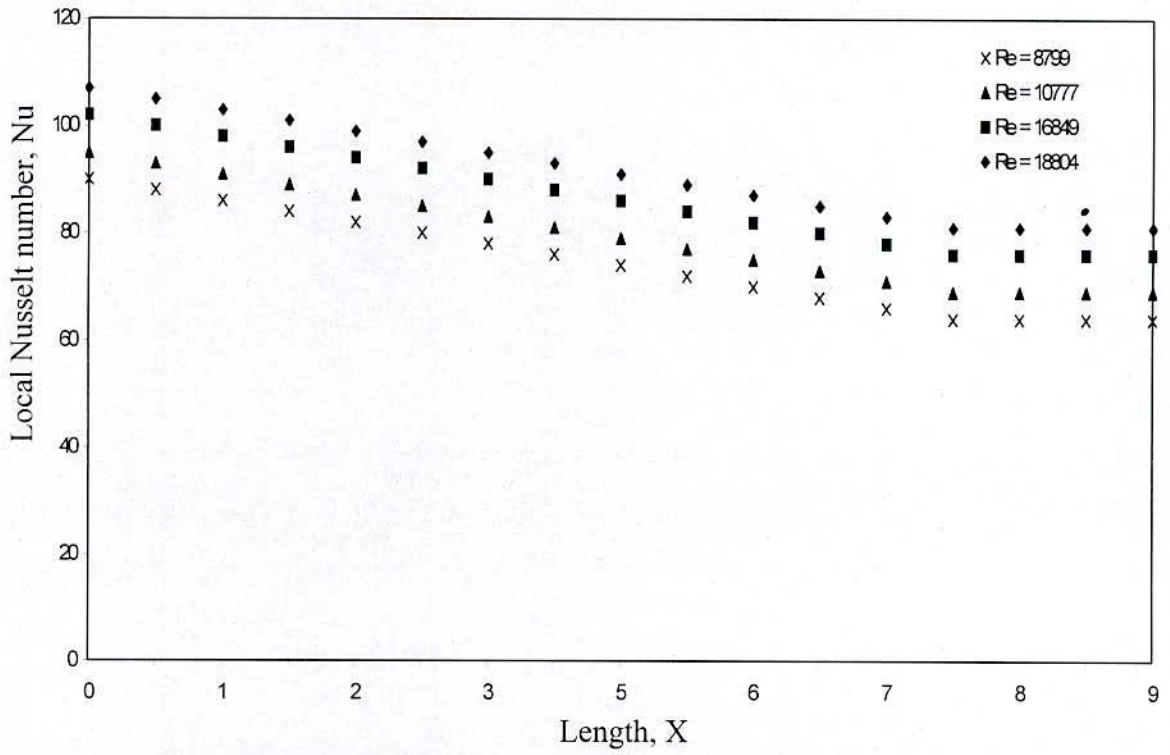


Figure 4.1.14. Distribution of local Nusselt Number over surface of roughness, $\epsilon = 0.01613$ at various jet exit Reynolds number.

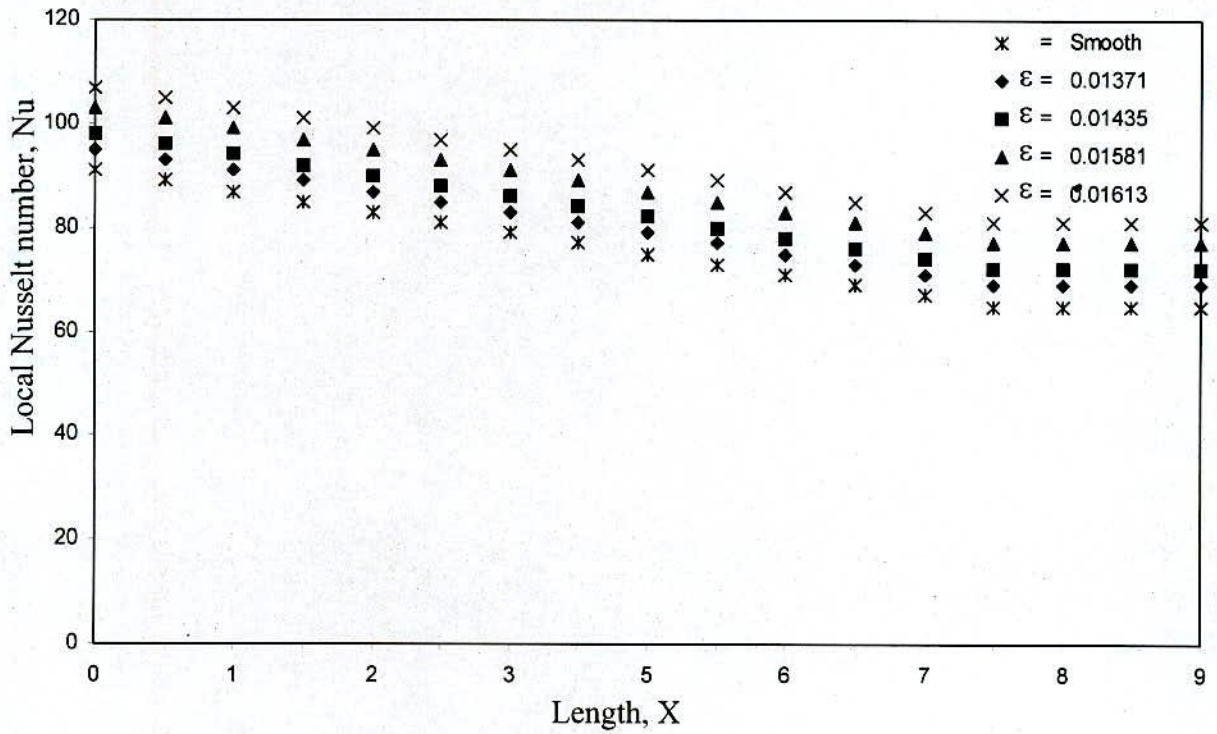


Figure 4.1.15. Distribution of local Nusselt Number of different surfaces at jet exit Reynolds number $Re = 18804$.

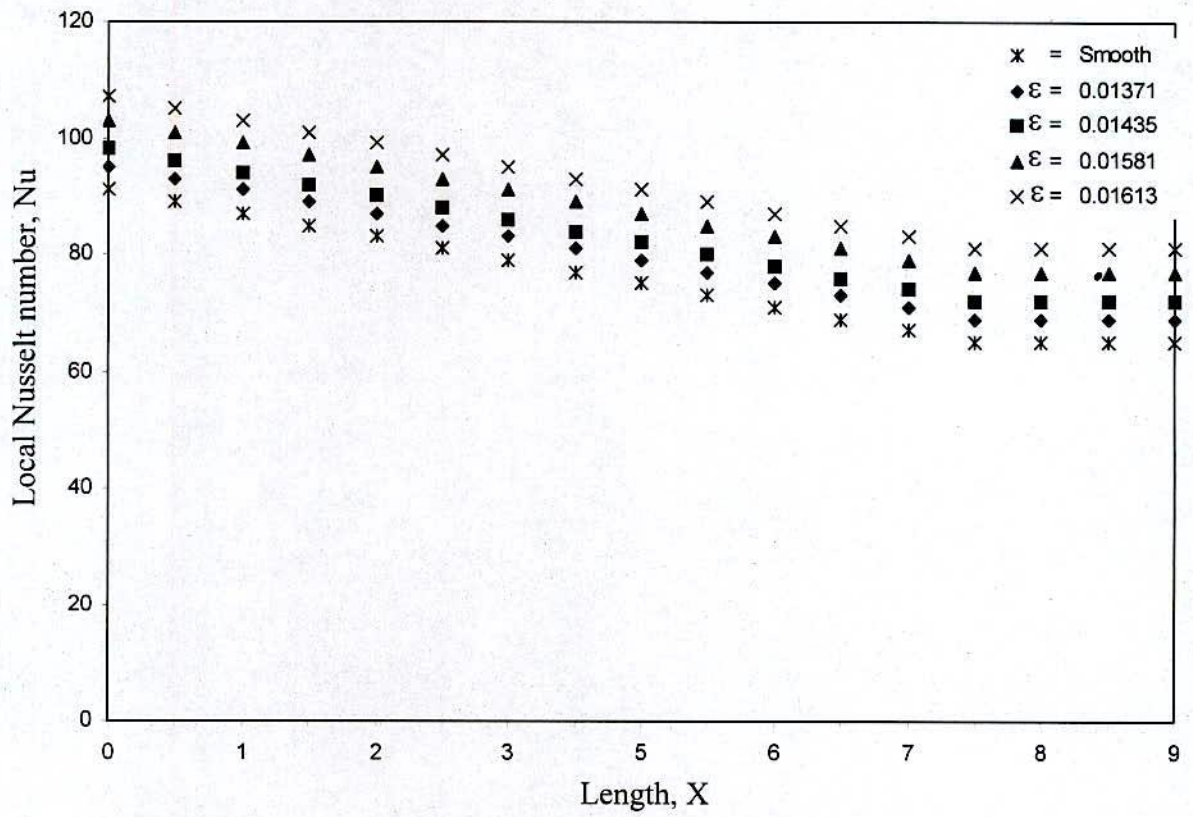


Figure 4.1.16. Distribution of local Nusselt Number different surface at jet exit Reynolds number $Re = 16849$.

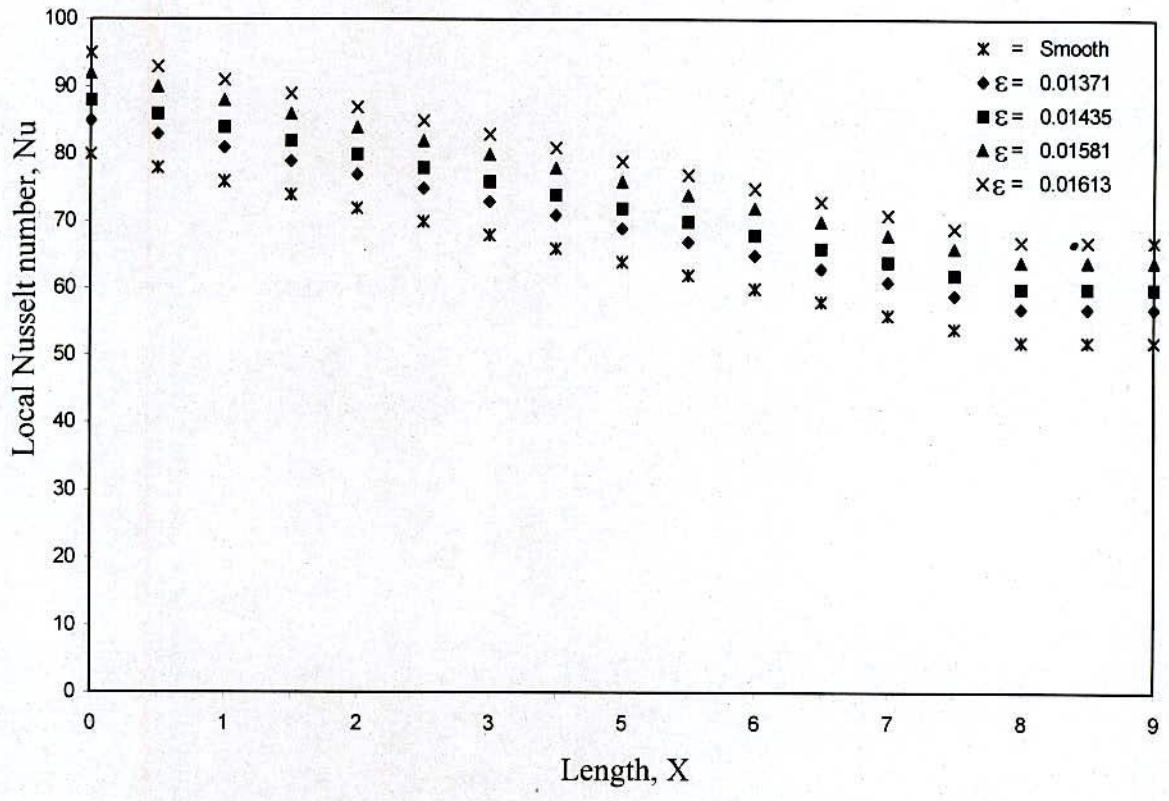


Figure 4.1.17. Distribution of local Nusselt Number over different surfaces at jet exit Reynolds number $Re = 10777$.

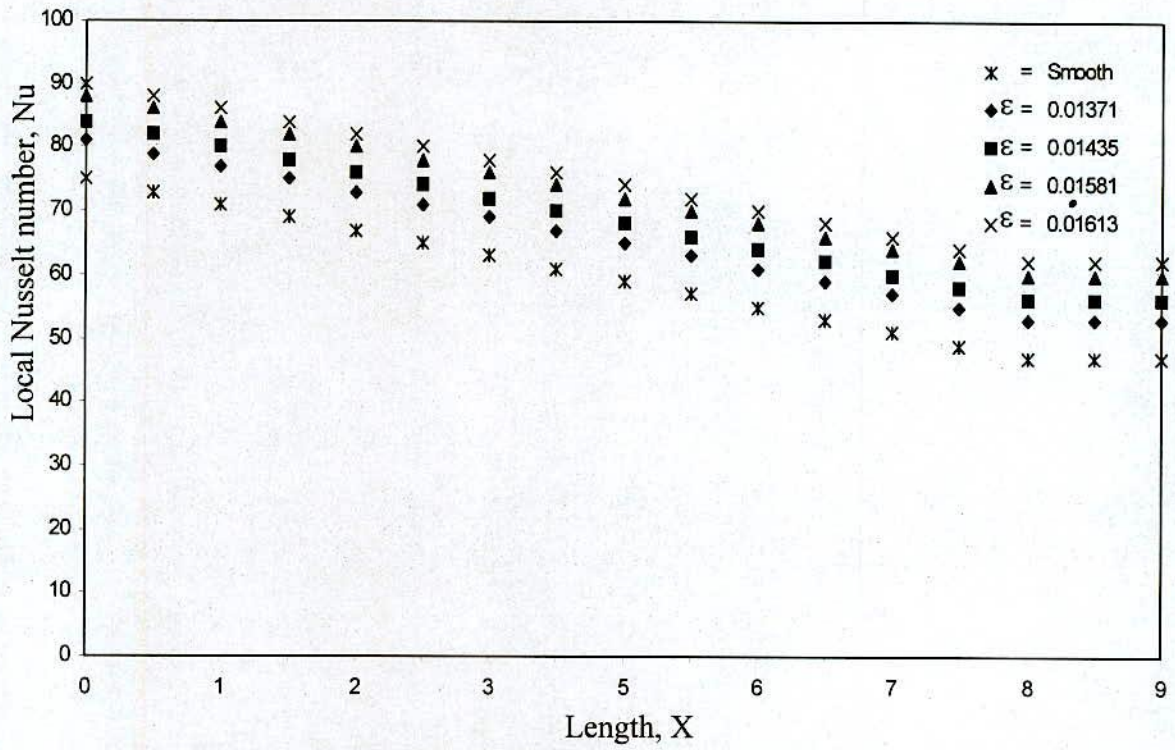


Figure 4.1.18. Distribution of local Nusselt Number over the surface at jet exit Reynolds number $Re = 8799$

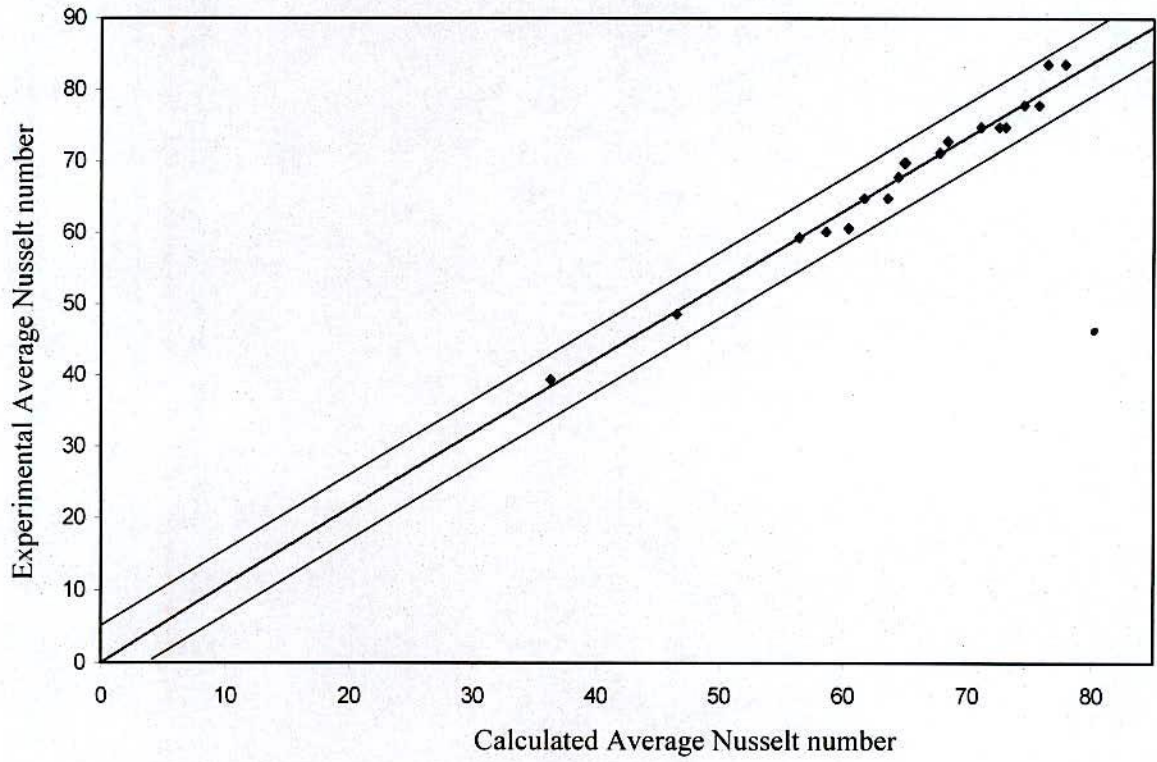


Figure 4.2 Calculated Average Nusselt number Vs. Experimental Average Nusselt number.

REFERENCES

1. G. Myers, J. J. Schaur, and R. H. Eustis, "Plane Turbulent Wall Jet Flow Development and Friction Factor," ASME Paper No. 62-Hyd-4, to be published in Trans. ASME.
2. J. Zerbe and J. Selna. "An Empirical Equation for the Co-efficient of Heat Transfer to a Flat Surface From a Plane Heated Air Jet Directed Tangentially to the Surface." NACA TN 1070, 1946.
3. M. Jadbabadi, R. L. Rose and M. Spielman, "Heat Transfer From an Air Jet to a Plane Plate With Entrainment of Water Vapor From the Environment," Trans. ASME, Vol. 72, 1950, PP/ 859.
4. R.C. Bergh, H. Wittner, F. Donnally and M. Martin, "Heat Transfer and velocity Distribution Characteristics to a Free Jet Discharged From a Narrow Slot and Directed Parallel to a Horizontal Plate," Republic Aviation Report ERF-3. 1945.
5. J.P. Hartnett, R.C. Birkebak and E. R. G. Eckert. "Velocity Distributions, Temperature Distributions, Effectiveness and Heat Transfer for Air Injected Through a Tangential slot in to a turbulent Boundary Layer," JOURNAL of Heat Transfer, Trans. ASME. Series C. vol. 83, 1961, PP/ 293-306.
6. R. A. Seban "Heat Transfer and Effectiveness for a Turbulent Boundary Layer with Tangential fluid injection." JOURNAL of Heat Transfer, Trans. ASME, Series C. vol. 82, 1960, PP/ 308-312.
7. R. A. Seban and L. H. Back. "Velocity and Temperature Profiles in Turbulent Boundary Layers with Tangential Injection." Journal of Heat Transfer. Trans. ASME Series C. vol. 84. 1962. PP/45-54.
8. R. A. Bajura and Albin A Szewczyk "Experimental Investigation of a Laminar Two-Dimensional Plane Wall Jet", J. Phys. Fluid, vol. 13, No. 7, PP/1653-1664, July, 1970.
9. Miyazaki, h. and Silberman, E., " Flow and heat transfer on a flat plate normal to a two-dimensional laminar jet issues from a nozzle

- to finite height.”, Int. J. Heat and Mass transfer, vol. 15, PP/2097-2107, 1972.
10. A. J. Hogg, H. E. Huppert and W. B. Dade, “Erosion by planar turbulent wall jets” J. fluid Mech., vol. 338, PP/317-340, 1997.
 11. Yohei Sato, Koichi Hishida and Masanobu Maeda, “Effect of Dispersed Phase on Modification of Turbulent flow in a Wall Jet.” J. of Fluids Engineering vol.118, PP/307-315,1996.
 12. F. J. Higuera, “Opposing mixed convection flow in a wall jet over a horizontal plate.” J. Fluid Mech., vol.342, PP/355-375, 1997.
 13. M. E. Stern, E. P. Chassignet and J. A. Whitehead, “The wall jet in a rotating fluid” J. Fluid Mech., vol.335. PP/1-28, 1997.
 14. M. D. Zhou, C. Heine and Wygnansk, “ The effects of excitation on the coherent and random motion in plane wall jet” J. Fluid Mech. vol.310. PP/1-37,1996.
 15. D. Roy and S. R. Bhattacharya, “ Study of the variation of skin friction coefficient with roughness” Proceedings of the fifth Annual Paper Meet, IEB, Mech, Engg. Division, PP/28-36,1998.
 16. V.Kuppu Rao, “ A note on mass transfer in turbulent wall jets” Int. J. Heat and mass transfer, vol. 23, PP/1690-1693, 1980.
 17. G. P. Hammond, “Complete velocity profile and ‘Optimum’ Skin Friction Formulas for the plane wall jet”, J. Fluid Engg. vol. 104, PP/59-66,1982.
 18. Gardon, R. and Akfirat, J.C. 1965. “The role of turbulence in determining the heat transfer characteristics of impinging jets.” International Heat transfer conference. PP/1261-1272.
 19. Goldsten, R.J. and Bhabhani, A.I. “Impingement circular jet with and without cross-flow.” International journal of Heat and Mass transfer, Vol-25, PP/1377-1382.

20. Jambunathan, K.L. et al, 1992, "A review of heat transfer data for single circular jet impingement." International journal of heat and fluid flow. vol-13, PP/106-115.
21. Bouchez., J.P. and Goldesten, R.J., 1995. "Impingement cooling from a circular jet in a cross-flow." Int. journal of heat and mass transfer vol-18. PP/719-730.
22. Sparrow, E.M. et al, 1975, "Effect of nozzle surface separation distance on impingement heat transfer for a jet in a cross flow." ASME journal of heat transfer, vol-97, PP/528-533.
23. Huang, L. and EL-Gank, M.S. 1994. Heat transfer of an impinging jet on a flat surface International journal of heat and mass transfer, vol-37, PP/1915-1923.
24. Huber, A.M. and Viskent. R., 1994, "Effect of jet-spacing on convective heat transfer to confined, impinging array of axisymmetric air jet." International journal of heat and mass transfer. vol-37. PP/2859-2869.
25. Hollworth, B.R. and Gero, L.R., 1985, "Entertainment effects on impingement heat transfer: part-2-local heat transfer measured." ASME journal of heat transfer, vol-107, PP/910-915.
26. Steven, J and Webb, B.W., 1991, "Local heat transfer coefficients under an axisymmetric, single phase liquid jet." ASME journal of heat transfer, vol-113, PP/71-78.
27. Garmilla, S.V. and Rice, M.A., 1995, "Confined and Submerged liquid jet impingement heat transfer." ASME journal of heat transfer. Vol-117. PP/871-877.
28. Jung-Yang san et al., 1997, "Impingement cooling of a confined circular air jet." International journal of heat and mass transfer, val-40, no-6, PP/1355-1364.
29. Ali khan, M.M., kagasi, K., Hirata, M., and Nushiwaki, 1982, "Heat transfer augmentation in an axisymmetric impinging jet," Proceedings, 7th Int. Heat transfer conference, paper FC 6-3. PP/363-368.



30. Hrycak. p., 1984, "Heat transfer from impinging jets to a flat plate with conical and ring protuberances. "International journal of heat and mass transfer. vol.-27. PP/2145-2154.
31. Obot. N.T. and Trabold, T.A., 1987, "Impingement heat transfer within arrays of circular jets: part-2, effects of cross-flow in the presence of roughness elements, Trans. ASME journal of Turbomachinery, vol-109, PP/594-601.
32. Hansen. L.G. and Webb, B.W., 1993, "Air jet impingement heat transfer from modified surfaces." International journal of Heat and mass transfer, vol-1-36.no.-4, PP/989-997.
33. Hossain, K.A. and Arora, R.C., 1997," Flow characteristics of laminar slot jet impinging over a circular cylinder." Proceedings, 4th annual paper meet I.E.B. Mech. division, Paper no.-6, PP/51-57.
34. Ali, M.A.T., Hassan, A., and Islam, M.T. "Turbulent boundary layer growth on a step changed smooth to rough surface." proceedings, 2nd annual paper meet, I.E.B., PP/106-122.
35. Md. Nurul Islam, " Impingement Heat Transfer Due To Circular Air Jet Over Rough Flat Surfaces." Project paper, Mech. Engg. Dept. BIT. Khulna, 2000.
36. Hollworth, B.R. and durbin, M., 1989, "Impingement cooling of electronics." National heat transfer conference. HTD. vol-11. PP/89.
37. Hamadah, T.T., 1989, "Air jet impingement cooling of an array of simulated electronics packages." Proceedings, national heat transfer conference, HTD. col-111. PP/097-105.
38. Donaldson, C.D., Sndeker, R.S. And Margolis, D.P., 1971. "Astidy of free jet impingement. Part-2. Free jet turbulent structure and impingement heat transfer." Journal of Fluid mechanics. Vol-45. PP/477-512.
39. Gorshkov,G.I., 1984, "Near wall turbulence in jet impingement on a wall." Journal of applied mechanics, Tech. Physics. col-25.PP/233-241.

40. Kataoka, K. and Misushina, T., 1974, "Local enhancement of the rate of heat transfer in an impinging round jet by free-stream turbulence." proceedings of 5th international heat transfer conference, vol-2, paper-FC8,3. PP/305-309.
41. Mihita, 1987, "The effect of surface renewal due to large scale eddies on jet impingement heat transfer." International journal of heat and mass transfer, vol-30, PP/559-567.
42. Popiel, C.O. and Trass, O., 1982, "The effect of ordered structure of turbulence on momentum, heat and mass transfer of impinging round jets." Proceedings of 7th international conference of heat transfer. vol-6, PP/141-146.
43. Webb, B.W. and Lyte, D., 1994, "Air jet impingement heat transfer at low nozzle-plate spacing." International journal of heat and mass transfer. Vol-37, PP/1687-1697.

Appendix – A

Sample Calculation

Method of Calculation :

Data were obtained to report average Nusselt number, \bar{Nu} as a function of jet Reynolds number, Re , relative roughness, ϵ . But jet Reynolds number, Re , Surface roughness, Ra , Local and Average Nusselt number, Nux and \bar{Nu} were Calculated by the following methods.

Calculation of Reynolds number :-

$$\text{Specific weight of Air} = \gamma_{\text{air}} = \rho \times g = 1.12 \times 9.81 = 10.98 \text{ N/m}^2$$

$$\text{Specific gravity of the manometric fluid} = 0.784$$

$$\text{So, specific weight of manometric fluid, } \gamma = 9810 \times 0.784$$

$$= 7691 \text{ N/m}^3$$

$$\text{Kinematic viscosity of air, } \gamma = 1.45 \times 10^{-5} \text{ m}^2/\text{sec.}$$

$$\text{Reading from inclined manometer} = \Delta P$$

$$\text{So pressure head, } h_p = \frac{fP}{\gamma_{\text{air}}}$$

$$\text{Velocity of air, } V = \sqrt{2gh_p}$$

$$\text{Reynolds number (Re)} = \frac{Vd}{\gamma}$$

Calculation of surface roughness :-

$$\text{Center line average (Ra) in micrometer} = \frac{h_1 + h_2 + h_3 + \dots + h_n}{n}$$

where, $h_1, h_2, h_3, \dots, h_n$ are ordinates measured on both sides of the mean line and n is the number of ordinates.

$$\text{Relative roughness, } \epsilon = \frac{Ra}{d}$$

Calculation of Nusselt number :-

$$\text{Dimensionless temperature, } \dot{A} = \frac{(T - T_j)}{(T_w - T_j)}$$

Where, T = local temperature after impingement

T_j = Temperature of air at jet exit.

T_w = Wall (plate) temperature at steady state.

$$\text{Heat flux, } q = \frac{-k_s (T_2 - T_1)}{dx}$$

Here, $k_s = 54 \text{ w/m.K}$ for Mild Steel (of 0.5% c) at 100°C .

Thus, Average heat flux, $q = 4016.25 \text{ W/m}^2$.

$$\text{Local Nusselt number, } Nu_x = \frac{q \cdot dx}{k_a (T - T_j)}$$

Here, $dx = 0.0062 \text{ m}$.

k_a = Thermal conductivity of air at 30°C .

$$= 0.026 \text{ w/m.K}$$

$$\text{Average Nusselt number, } \overline{Nu} = \frac{\sum Nu_x \cdot x}{L}$$

Calculation of Correlation :

The correlation for Average Nusselt number has been developed in terms of jet Reynolds number (Re), relative roughness (ϵ), by the formula $\overline{Nu} = c Re^n \epsilon^m$. By least square method the constants, c, n and m of the above equation was calculated.

Uncertainty Analysis :

A more precise method of estimating uncertainty in experimental results has been presented by Kline and McClintock. The method is based on a careful specification of the uncertainties in the various primary experimental measurements. The result R is a given function of the independent variables $x_1, x_2, x_3 \dots, x_n$. Thus,

$$R = R(x_1, x_2, x_3 \dots, x_n)$$

Let W_R be the uncertainty in the result and w_1, w_2, \dots, w_n be the uncertainties in the independent variables. If the uncertainties in the independent variables are all given with same odds, then the uncertainty in the result having these odds is given as

$$w_R = \left[\left(\frac{\partial R}{\partial x_1} w_1 \right)^2 + \left(\frac{\partial R}{\partial x_2} w_2 \right)^2 + \dots + \left(\frac{\partial R}{\partial x_n} w_n \right)^2 \right]^{1/2}$$